# Physical Properties of Polymers Handbook

James E. Mark

*Polymer Research Center and*
*Department of Chemistry*
*University of Cincinnati*
*Cincinnati, Ohio*

AIP PRESS

American Institute of Physics Woodbury, New York

# CHAPTER 28

# Gels

Ferenc Horkay and Gregory B. McKenna

*Polymers Division, National Institute of Standards and Technology, Gaithersburg, MD 20899*



## 28.1 INTRODUCTION

When long polymer molecules are chemically linked together to form a three-dimensional network, the resulting material exhibits a unique set of properties that have come to be referred to as "rubber-like." Among these are large deformation elasticity which has important consequences for mechanical behavior and resistance to solvent attack. As for the latter, when solvent molecules penetrate into the polymer, it undergoes swelling rather than dissolution, and the diluted network is referred to as a chemically crosslinked gel. While there are several structures that exhibit gel-like behavior (e.g., (1) covalent networks of long chain molecules, (2) physical networks formed by aggregation of polymer chains (gelatin, agarose), (3) lamellar, fibrillar or reticular systems exhibiting partially ordered structures (clays, surfactants, etc.), the focus of this work is solely on elastomeric polymer networks containing a three-dimensional permanent structure of high molecular weight chain molecules swollen in a low molecular weight diluent as depicted in Fig. 28.1.

The covalent network, composed of long flexible chains capable of adopting large conformational changes (chain deformations), extends throughout the sample providing the ability to undergo large and reversible (elastic) deformations and a corresponding ability to swell rather than dissolve. Though the molecular origins of rubber elasticity were recognized as early as the 1930s and 40s [1–5], a complete theoretical description of the swelling behavior of rubber-like polymers has yet to be achieved. The result is that while there is a general understanding of the behavior of crosslinked materials within the framework of some "classical" models of rubber elasticity, there are still several unresolved problems. For example, even the fundamental assumption, originally put forth by Frenkel [5], Flory and Rehner [2,4] that the free energy of mixing of a solvent and rubber network can be separated into an elastic term for the network and a mixing term for the solvent and polymer is a subject for much recent research and discussion [6–32].

There is a diversity of theoretical models used to elucidate the relationships between the molecular parameters of the network and the various experimental results [33–57]. Hence, the resulting deduction of the molecular structure of the network can depend on the model chosen for data analysis. Additionally, the structure of the networks at the supermolecular level is a function of the preparation conditions (temperature, concentration at crosslinking, chemical nature of the crosslinker, etc.). During network formation, imperfections in the structure may also develop. In many cases the crosslinking process leads to fixation of otherwise nonequilibrium states. A wide variety of molecular superstructures may be produced within networks prepared from the same starting materials. This makes comparisons of experimental results from different literature sources complicated. Consequently, a simple tabulation of previously published data is not particularly useful.

The present work is intended to briefly survey the basic thermodynamic considerations of rubber elasticity and swelling from both a continuum point of view and with regard to existing network models. Our goal is to illustrate the range of applicability and the limitations of the different approaches for the description of experimental data. Addi-

tionally, this work should provide the reader with the ability to use the models to obtain estimates of the molecular structure of the gel through analysis and interpretation of typical sets of experimental data. Conversely, the swelling and mechanical response of new networks should be able to be estimated from a chemist's knowledge of the molecular parameters of the network.

## 28.2 THEORETICAL BACKGROUND

### 28.2.1 General Considerations

In thinking about the behavior of rubber networks and gels, there are two features of behavior that we consider in the following. First, the fundamental nature of the elastomeric network itself in the undiluted state needs to be weighed. This is done using both the phenomenological theories of rubber elasticity and the molecular (statistical mechanical) models. Both approaches result in forms of the free energy function (Helmholtz) of the network and ultimately need to give the same descriptions of the phenomenological behavior of the dry network. Second, we consider the specific behavior of the swollen network or gel from similar considerations. In the latter case, the formulation of a mixing free energy as a function of the swelling ratio is also required in addition to the elastic free energy.

Laboratory measurements, for the most part, record the macroscopic behavior of the material. Depending on the purposes of the experimenter, the link between the molecular models and the phenomenological models provides a basis for either deducing molecular parameters from the measurements or for predicting future measurements from known molecular structures. The latter is primarily important to estimate the physical properties of a given gel whose molecular structure is known. The background provided in what follows should permit one to do both within the limitations of current knowledge.

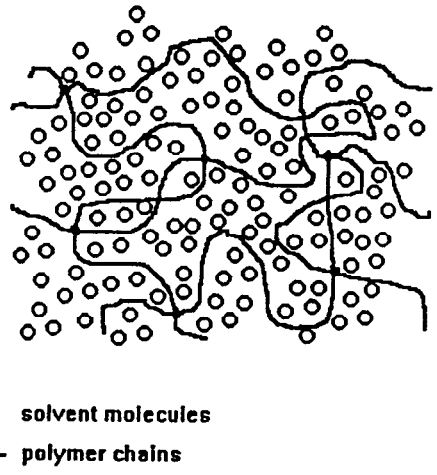


**FIGURE 28.1.** Schematic representation of a chemically crosslinked polymer network swollen by a low molecular weight solvent.

### 28.2.2 The Strain Energy Density Function—The Mechanical Contribution to the Helmholtz Free Energy

*Continuum Description*

There is an extensive body of literature describing the stress-strain response of rubber-like materials that is based upon the concepts of the Finite Elasticity Theory which was originally developed by Rivlin and others [58,59]. The reader is referred to this literature for further details of the relevant developments. For the purposes of this chapter, we discuss the development of the so-called Valanis–Landel Strain Energy Density Function (VL function) [60], because it is a form that is most commonly derived from the statistical mechanical models of rubber networks and has been very successful in describing the mechanical response of crosslinked rubber and it is resultingly very useful in understanding the behavior of swollen networks.

Here we begin with a sample of rubber having initial dimensions $l_1, l_2, l_3$. We deform it by an amount $\Delta l_1, \Delta l_2, \Delta l_3$ and define the stretch (ratio) in each direction as $\lambda_i = (l_i + \Delta l_i)/l_i = l/l_i$. The purpose of the Finite Elasticity Theory has been to relate the deformations of the material to the stresses needed to obtain the deformation. This is done through the Strain Energy Density Function, which we describe using the Valanis–Landel formalism as $W(\lambda_1, \lambda_2, \lambda_3)$. Importantly, as we will see later, this is the mechanical contribution to the Helmholtz Free Energy. Valanis and Landel assumed [60] that the strain energy density function is a separable function of the stretches $\lambda_i$:

$$W(\lambda_1, \lambda_2, \lambda_3) = w(\lambda_1) + w(\lambda_2) + w(\lambda_3) + a \ln(\lambda_1 \lambda_2 \lambda_3). \tag{28.1}$$

While the term $a\ln(\lambda_1\lambda_2\lambda_3)$ is not important in the mechanical response, because of the incompressibility assumption, it may be important in swelling [61]. We also note that some of the molecular models include this logarithmic term. Then, the principal stresses $\sigma_{ii}$ in any deformation can be related through the strain energy function and deformations as follows:

$$\sigma_{ii} - \sigma_{jj} = \lambda_i w'(\lambda_i) - \lambda_j w'(\lambda_j), \tag{28.2}$$

where $w'(\lambda) = dw(\lambda)/d\lambda$ is the derivative of the VL function $w(\lambda)$. We note that the stresses are the true stresses in that they referred to the deformed sample geometry. In the dry, unswollen rubber, the material is generally assumed to be incompressible, meaning that the distortional or shape-changing deformations are much more easily made than are the volume-changing ones, so that the latter can be neglected. Hence Eq. (28.2) is written in terms of the principal stress differences. In the case of a uniaxial deforma-

tion $\lambda$ in the 1 direction, Eq. (28.2) becomes:

$$\sigma_{11}-\sigma_{22}=\lambda_1 w'(\lambda_1)-\lambda_2 w'(\lambda_2), \qquad (28.3)$$

and because of the incompressibility condition that $\lambda_1\lambda_2\lambda_3=1$ we find that $\lambda_2=\lambda_3=\lambda_1^{-1/2}$ and Eq. (28.3) becomes:

$$\sigma_{11}-\sigma_{22}=\lambda w'(\lambda)-\lambda^{-1/2}w'(\lambda^{-1/2}), \qquad (28.4)$$

where $\lambda=\lambda_1$. For uniaxial extension, $\lambda>1$, while for uniaxial compression, $\lambda<1$.

From a practical viewpoint, Eq. (28.4) can be used to describe the stress-strain relation of a material if $w'(\lambda)$ is known. $w'(\lambda)$ can be obtained in the laboratory in various ways, such as pure shear experiments as described by Valanis and Landel [60] by torsional measurements as described by Kearsley and Zapas [62] and by a combination of tension and compression experiments as also described by Kearsley and Zapas [62]. Treloar *et al.* [63] have also shown that the VL function description of the mechanical response of rubber is a very good one. The reader is referred to the original literature for these methods.

Another point to keep in mind here is that in most models, the description of rubber elasticity given from statistical mechanical models results in a Valanis–Landel form of the Strain Energy Density Function. This becomes important in the following developments. We now look at some common representations of the strain energy density function used to describe the stress-strain behavior of crosslinked rubber.

There are two common phenomenological strain energy density functions that have been used to describe the stress-strain response of rubber [58,59,64]. These are referred to as the Neo-Hookean form and the Mooney–Rivlin form and both can be written as Valanis–Landel forms, although they represent truncated forms of more general strain energy density functions. The Neo-Hookean form is a special form of the Mooney–Rivlin form, so we will begin with the latter. For a Mooney–Rivlin material the Strain Energy Density Function is written as:

$$W(\lambda_1,\lambda_2,\lambda_3)=C_1(\lambda_1^2+\lambda_2^2+\lambda_3^2-3)+C_2(\lambda_1^{-2}+\lambda_2^{-2}+\lambda_3^{-2}-3), \qquad (28.5)$$

and we see that the VL function for this is of the form $w(\lambda_i)=C_1\lambda_i^2+C_2\lambda_i^{-2}$ and the VL derivative is given as:

$$w'(\lambda_i)=2C_1\lambda_i-2C_2\lambda_i^{-3}, \qquad (28.6)$$

where $C_1$ and $C_2$ are material constants, often referred to as the Mooney–Rivlin Coefficients. For uniaxial deformations of magnitude $\lambda$ one then writes Eq. (28.4) for the Mooney–Rivlin stress-strain response as:

$$\sigma_{11}-\sigma_{22}=(\lambda^2-1/\lambda)\{2C_1+2C_2/\lambda\}. \qquad (28.7)$$

Equation (28.7) makes obvious the reasons for the representation of experimental data in the so-called Mooney–Rivlin plot. If the material has a Mooney–Rivlin strain energy density function then a plot of $(\sigma_{11}-\sigma_{22})/(\lambda^2-1/\lambda)$ vs. $1/\lambda$ results in a straight line with the slope and intercept at $\lambda=1$ determining $2C_2$ and $(2C_1+2C_2)$, respectively.

For the Neo-Hookean material, the strain energy density function is the same as for the Mooney–Rivlin material but with $C_2=0$:

$$W(\lambda_1,\lambda_2,\lambda_3)=C_1(\lambda_1^2+\lambda_2^2+\lambda_3^2-3). \qquad (28.8)$$

The VL derivative is:

$$w'(\lambda_i)=2C_1\lambda_i. \qquad (28.9)$$

The corresponding reduced stress $\sigma_R$ is:

$$\sigma_R=(\sigma_{11}-\sigma_{22})/(\lambda^2-1/\lambda)=2C_1. \qquad (28.10)$$

Hence, in the Mooney–Rivlin plot, the stress-strain data are reduced to a line of slope zero.

A point worth noting here is that several of the molecular models that are described in the subsequent sections are Neo-Hookean in form. Normally, dry rubbers do not exhibit Neo-Hookean behavior. As for the Mooney–Rivlin form of strain energy density function, rubbers may follow such behavior in extension, yet they do not behave as Mooney–Rivlin materials in compression. In Fig. 28.2, we depict typical experimental data for a poly(dimethylsiloxane) network [39] and compare the response to Mooney–Rivlin and Neo-Hookean behaviors. The horizontal lines represent the affine and the phantom limits (see the Network Models section). The straight line in the range $\lambda^{-1}<1$ shows the fit of the Mooney–Rivlin equation to the experimental data points.

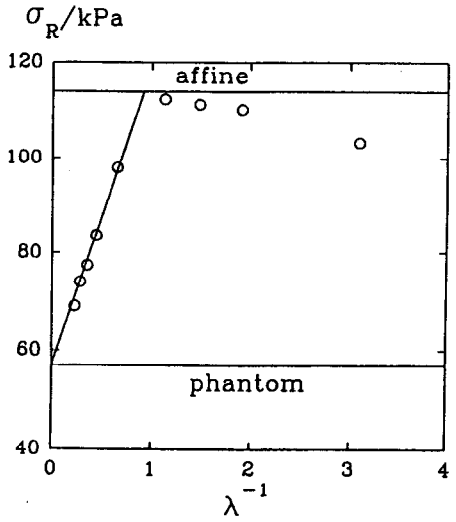


**FIGURE 28.2.** Comparison of typical stress-strain data for PDMS rubber [39] in a "Mooney–Rivlin" plot with "Neo-Hookean" and "Mooney–Rivlin" strain energy function descriptions. (See text for discussion.)

## *Statistical Theories*

### *Structural Characteristics of Polymer Networks*

In this section we discuss the most important structural parameters characteristic of an ideal polymer network. The structure of a real network always displays deviation from that of an ideal network. Network defects, such as unreacted functionalities, cyclic structures, and entanglements, arise from the statistics of the crosslinking process. The crosslinking reaction, in general, results in a length distribution for the network chains. In addition to the molecular imperfections, real networks always contain inhomogeneities, i.e., regions in which the polymer concentration is permanently higher than the average concentration. The topological structure of any real network is very complex and no complete theoretical treatment is available at the moment. It is worthwhile, however, to define the structural parameters for a perfect network because it allows us to treat any real network by reference to these parameters. Statistical models yield explicit expressions for the relation between the molecular structure of the network and the elastic properties.

The most important molecular parameter characteristic of a polymer network is the concentration of the elastic chains or that of the elastically active junctions connecting the macromolecules. An active junction is joined by at least three paths to the polymer network and an active chain is defined as one terminated by active junctions at both ends. There are several ways to express the extent of crosslinking: (1) the concentration of the elastically active chains, $\nu_{el}/V_0$, where $\nu_{el}$ is the number of chains connecting two elastically active junctions and $V_0$ is the volume of the dry network; (2) the molecular weight of the polymer chains between the junctions

$$M_c = \rho(V_0 N_A / \nu_{el}), \tag{28.11}$$

where $\rho$ is the density of the polymer and $N_A$ is Avogadro's number; (3) the crosslink density, $\mu_{el}/V_0$, where $\mu_{el}$ is the number of the crosslinks; and (4) the cycle rank density, $\xi/V_0$, where $\xi$ is the cycle rank, i.e., the number of independent circuits in the system. Naturally, these quantities are not independent. The relationship between $\nu_{el}$, $\mu_{el}$ and $\xi$ for a "perfect" network is given by [35]

$$\xi = \nu_{el} - \mu_{el} + 1. \tag{28.12}$$

In Fig. 28.3 a network structure is shown with $\xi=4$, $\nu_{el}=12$ and $\mu_{el}=9$.

Another important parameter is the crosslink functionality, $f$, which is the number of chains emanating from a network junction. Only junctions with functionality higher than 2 are elastically active. For perfect networks, i.e., crosslinked polymers containing no defects, $\nu_{el}$ and $\mu_{el}$ are connected by the functionality of the crosslinks [65]

$$\mu_{el} = (2/f)\,\nu_{el}. \tag{28.13}$$

Real networks always contain molecular imperfections, such as pendant chains bound to the network at one end only, intramolecular loops formed by the linking of two units of the same chain, and intermolecular entanglements. For an imperfect tetrafunctional network Flory [66] proposed a simple formula for correction for pendant chains

$$\nu_{el} = \nu_0(1 - 2M_c/M_n), \tag{28.14}$$

where $\nu_0$ is the total number of chains in the network, and $M_n$ is the number average molecular weight of the primary molecules.

The extent to which entanglements contribute to network elasticity is not yet fully resolved. In the model of Langley [45], Dossin, and Graessley [46–48] a contribution to the equilibrium modulus is associated with the plateau modulus of viscoelasticity. On the other hand, Flory [36] and Erman [38–40] assume that interpenetration of chains is solely reflected by suppression of the fluctuations of junctions.

A further type of network defect is caused by inhomogeneities. Clustering of chains or network junctions causes permanent departures from the homogeneous distribution of the polymer throughout the gel. Regions of higher polymer concentration build-up that appear as permanent deviations from uniformity. They are specific to the given system and dependent upon the condition of crosslinking. The effect of inhomogeneities on the elastic and swelling behavior of the networks has not been considered quantitatively in any theoretical model of rubber elasticity.

### *Network Models*

The primary goal of a general statistical theory is to derive an equation of state for the elastomeric molecular network which will hold for any deformation including swelling. Since the major contribution to the elasticity is

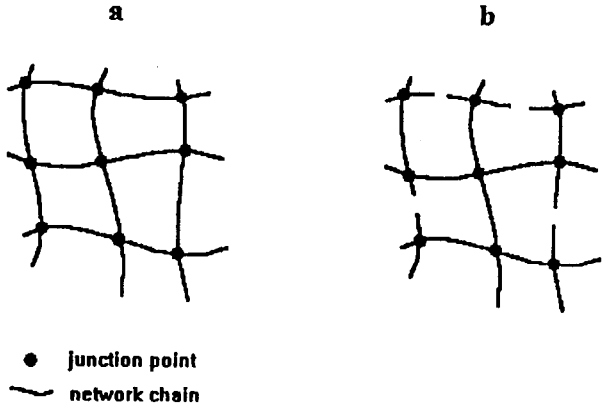


**FIGURE 28.3.** Schematic representation of a network structure with $\nu_{el}=12$, $\mu_{el}=9$ and $\xi=4$ (a). Note that the cycle rank is the number of cuts needed to reduce the network to a tree (b).

entropic, the molecular interpretation depends on how the stress affects the conformational distribution of an assembly of chains. The successful statistical model will provide predictive relationships between the molecular structure and topology of the network and its macroscopic behavior, e.g., mechanical and swelling responses.

The classical theories of rubber elasticity rest on two basic assumptions [4]

1. The elastic free energy of the network is the sum of the elastic free energies of the network chains, i.e., the interactions between the constituent chains are independent of the state of deformation, and do not make any contribution to the elastic free energy; and
2. The end-to-end distribution of the network chains is Gaussian, i.e., the excluded volume interactions are ignored.

The affine and the phantom models derive the behavior of the network from the statistical properties of the individual molecules (single-chain models). In the more advanced constrained junction fluctuation model the properties of these two classical models are bridged and interchain interactions are taken into account. We remark for completeness that other molecular models for rubber networks have been proposed [67–79], however these are not nearly as widely used and remain the subject of much debate. The reader is referred to the literature for further information on these models.

*The Affine Model.* In this model it is assumed that the displacement of the mean positions of the junctions and of the end-to-end vectors of the chains are transformed affinely, i.e., linearly in the macroscopic strain [80,81]. Fluctuations of the network junctions are completely suppressed by intermolecular entangling with neighboring coils sharing the same region of space. The elastic free energy of the affine network is given by [80–82]:

$$\Delta F_{el}^{aff}/kT=(\nu_{el}/2V_0)(\lambda_1^2+\lambda_2^2+\lambda_3^2-3) -(\mu_{el}/V_0)\ln(\lambda_1\lambda_2\lambda_3), \qquad (28.15)$$

where $\nu_{el}$ and $\mu_{el}$ are the number of the elastic chains and junctions in the network, and $\lambda_1$, $\lambda_2$, and $\lambda_3$ are the principal deformation ratios. Here we note that the affine model is of the Neo-Hookean form with $C_1=\nu_{el}/2V_0$, if there is no volume change upon deformation. Note also the presence of a logarithmic term in the free energy expression.

### *The Phantom Model*

In this model, polymer chains are allowed to move freely through one another and the network junctions fluctuate around their mean positions [3,83–85]. The conformation of each chain depends only on the position of its ends and is independent of the conformations of the surrounding chains with which they share the same region of space. The junctions in the network are free to fluctuate around their mean positions and the magnitude of the fluctuations is strain invariant. The positions of the junctions and of the domains of fluctuations deform affinely with macroscopic strain. The result is that the instantaneous distribution of the mean positions of the end-to-end vectors is not affine in the strain because it is the convolution of the distribution of the mean positions (which is affine) with the distribution of the fluctuations (which is strain invariant). The elastic free energy of deformation is given by

$$\Delta F_{el}^{ph}/kT=(\xi/2V_0)(\lambda_1^2+\lambda_2^2+\lambda_3^2-3), \qquad (28.16)$$

and again the free energy function is of the Neo-Hookean form, with $C_1=\xi/2V_0$.

*The Constrained Junction Fluctuation Model.* The affine and phantom models are two limiting cases on the network properties and real network behavior is not perfectly described by them (recall Fig. 28.2). Intermolecular entanglements and other steric constraints on the fluctuations of junctions have been postulated as contributing to the elastic free energy. One widely used model proposed to explain deviations from ideal elastic behavior is that of Ronca and Allegra [34] and Flory [36]. They introduced the assumption of constrained fluctuations and of affine deformation of fluctuation domains.

In the constrained junction fluctuation model [36,38–40] developed by Flory and Erman, the spatial fluctuations of the junctions are inhibited from the large values allowed in the phantom network by restrictions due to neighboring chains. The effect of conformational constraints are assumed to be imposed solely on the network junctions. The situation is illustrated by Fig. 28.4. The mean position of the network junction is located in point $A$. In a phantom network (Fig. 28.4a) the radius of the circle shows the average root-mean-square fluctuation $\langle(\Delta R)^2\rangle_{ph}^{1/2}$ around the mean position. The domain of constraints due to intermolecular interactions with neighboring chains and to steric

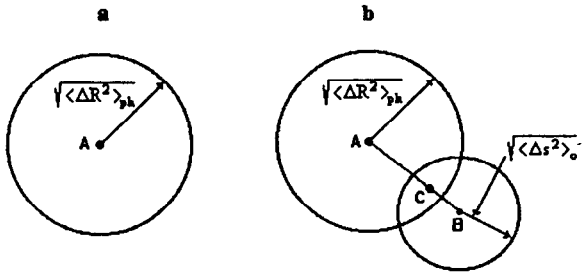


**FIGURE 28.4.** Effect of constraints on the fluctuations of network junctions. (a) Phantom model and (b) constrained junction fluctuation model. Note that the domain boundaries (circles in the figure) are diffuse rather than rigid. The action of domain constraint is assumed to be a Gaussian function of the distance of the junction from $B$ similarly as the action of the phantom network is a Gaussian function of $\Delta R$ from the mean position $A$.

requirements is represented by the smaller circle in Fig. 28.4b. This latter is centered at point $B$. Because of the effect of constraints, the mean position of the junction (i.e., the equilibrium position in the unstrained network) is removed from point $A$ to point $C$. The instantaneous position of the junction may differ significantly, however, from the equilibrium position because the junction fluctuates around its mean position. Thus, in addition to the phantom network contribution to the free energy, an important new parameter in this model is the measure of the severity of the constraints relative to those imposed by a phantom network

$$\kappa = \langle \Delta R^2 \rangle_{ph} / \langle \Delta s^2 \rangle_0, \tag{28.17}$$

where $\langle \Delta R^2 \rangle_{ph}$ is the mean-squared fluctuation in the positions of junctions from their mean locations in the phantom model, and $\langle \Delta s^2 \rangle_0$ is the mean-squared fluctuation around $B$ that would occur in the undeformed network if the junction were subject only to the effects of its interactions with the surrounding chains [86]. The range of $\kappa$ therefore is from 0 (phantom limit) to $\infty$ (affine limit). The size of the domains of constraints is assumed to decrease with increasing strain so that the junction fluctuations become larger. If the network is deformed the fluctuations become anisotropic in the stretching direction because the constraints become smaller.

The elastic free energy is given by [38–40]

$$\Delta F_{el} = \Delta F_{el}^{ph} + \Delta F_{el}^{c}, \tag{28.18}$$

where $\Delta F_{el}^{c}$ is the contribution to the elastic free energy arising from the presence of constraints relative to those in the phantom network $\Delta F_{el}^{ph}$ [see Eq. (28.16)]. This term can be written

$$\frac{\Delta F_{el}^{c}}{kT} = \left(\frac{\mu_{el}}{2V_0}\right) \sum_{t=1}^{3} [(1+g_t)B_t - \ln((B_t+1)(g_tB_t+1))], \tag{28.19a}$$

with

$$B_t = (\lambda_t - 1)(1 + \lambda_t - \zeta\lambda_t^2)(1+g_t)^{-2}, \tag{28.19b}$$

$$g_t = \lambda_t^2[\kappa^{-1} + \zeta(\lambda_t - 1)], \tag{28.19c}$$

where the parameter $\zeta$ characterizes the non-affine transformation of the domains of constraints with deformation.

Importantly, the model spans the behavior between the phantom and affine models. When $\kappa=\infty$ and $\zeta=0$ we recover the affine network behavior. In this case the junction fluctuations are completely suppressed, i.e., $\langle \Delta s^2 \rangle_0 = 0$. When $\kappa=0$, i.e., the junctions are free to fluctuate, we recover the phantom network model.

We note that the free energy function in the Flory–Erman model is a specific form of the Valanis–Landel Strain Energy Density Function. McKenna and Hinkley [61] determined the Valanis–Landel function for the junction constraint model

$$w'(\lambda_t) = \xi kT\lambda_t + (\mu_{el}kT/2)\{B_t^*(1+g_t) + g_t^*B_t - B_t^*(B_t + 1)^{-1} - (g_tB_t^* + B_tg_t^*)(g_tB_t+1)^{-1}\}, \tag{28.20}$$

where

$$B_t^* = B_t\{[2\lambda_t(\lambda_t - 1)]^{-1} + (1 - 2\zeta\lambda_t)[2\lambda_t(1 + \lambda_t - \zeta\lambda_t^2)]^{-1} + 2g_t^*(1+g_t)^{-1}\}, \tag{28.21}$$

and

$$g_t^* = \kappa^{-1} - \zeta(1 - 3\lambda_t/2) \tag{28.22}$$

We will come back to these models subsequently.

### *The Mixing Contribution to the Free Energy*

So far we have discussed the behavior of networks in the dry state. In the case of a swollen network, additional effects must be taken into account. The thermodynamics of mixing is governed by the interaction between the polymer and the solvent molecules. As we have seen in the section on network models, in gels the fluctuations of the network junctions are significantly altered by the presence of crosslinks. The formulation of a mixing free energy for the swollen network would require a detailed knowledge of the effect of osmotic forces on the size and shape of the fluctuation domains. This is beyond the scope of the existing molecular theories.

Because of the lack of an explicit molecular theory which accounts for the effect of crosslinking on the structure of a polymer solution, it is generally assumed that the functional dependence of the free energy of mixing in the swollen network is the same as in a polymer solution. Although this is a strong approximation, the application of the theoretical free energy functions derived for polymer solutions provides a simple and straightforward way to interpret the results of mechanical and swelling measurements performed on swollen polymer networks.

There are two essentially different ways to describe the thermodynamics of polymer solutions: classical (mean-field) theories [4] including recent renormalized models [87,88] and asymptotic scaling theories [89,90] based on the analogy found between critical phenomena and polymer chain statistics.

#### *Flory–Huggins Theory of Polymer Solutions*

The classical treatment of polymer solution thermodynamics due to Flory and Huggins [4] is based on a lattice model which assumes a uniform polymer segment concentration throughout the entire system. The free energy of mixing of a polymer solution is given by

$$\Delta F_{mix} = RT[n_1 \ln(1-\varphi) + n_2 \ln \varphi + \chi n_1 \varphi), \tag{28.23}$$

where $\varphi$ is the volume fraction of the polymer, $\chi$ is the Flory–Huggins interaction parameter, $n_1$ and $n_2$ are the numbers of moles of solvent and polymer, respectively. The

chemical potential of the solvent is defined as the derivative of the free energy of mixing with respect to amount of solvent

$$(\Delta\mu_1)_{mix}=(\partial\Delta F_{mix}/\partial n_1)=RT[\ln(1-\varphi)+(1-N^{-1})\varphi+\chi\varphi^2], \quad (28.24)$$

where $N$ is the degree of polymerization. For a crosslinked polymer $N=\infty$. In general, $\chi$ depends on the polymer concentration, [91] i.e.,

$$\chi=\chi_0+\chi_1\varphi+\ldots, \quad (28.24a)$$

where $\chi_0$ and $\chi_1$ are constants.

*Scaling Theory*

In the 1970s a new theory of polymers was developed based on the analogy found between polymer statistics and critical phenomena taking account of correlations between monomers [90]. For the chemical potential of mixing in the semi-dilute region scaling theory yields

$$(\Delta\mu_1)_{mix}=KRT\varphi^n \quad (\varphi^*<\varphi\ll 1), \quad (28.25)$$

where the prefactor $K$ is characteristic of the polymer/solvent system and the value of the exponent $n$ depends on the thermodynamic quality of the solvent. In a good solvent $n=2.31$, and in the theta condition $n=3$. $\varphi^*$ is the polymer volume fraction above which the domains of the coils start to overlap, i.e., the volume fraction of the polymer inside a separate coil

$$\varphi^*\propto N/R^3\propto N^{1-3\nu}, \quad (28.26)$$

where $\nu$ is the excluded volume exponent, the value of which is $\nu\simeq 3/5$ (good solvent condition) or $\nu=1/2$ (theta condition).

De Gennes proposed a description of the properties of swollen polymer networks based on the analogy found between the swollen network and semi-dilute polymer solutions ($\varphi^*$ theorem) [90]. The fully swollen gel is expected to maintain a polymer volume fraction, $\varphi_e$, which is proportional to the overlap concentration. In a good solvent

$$\varphi_e=z(f)\varphi^*\propto z(f)(1/2-\chi)^{-3/5}N^{-4/5}, \quad (28.27)$$

where $z(f)$ is a constant factor of the order of unity, $f$ is the crosslink functionality and $\chi$ is the Flory–Huggins polymer-solvent interaction parameter.

Many attempts to explain the results of osmotic and mechanical measurements on swollen polymer networks have invoked analogies with semi-dilute polymer solutions. Scaling forms for different physical quantities have been derived from the $\varphi^*$ theorem.

For example, the elastic (shear) modulus of a gel is given by [59]

$$G=B(\varphi_e/N_c), \quad (28.28)$$

where $\varphi_e$ is the volume fraction of the polymer in the fully swollen gel, $N_c$ is the degree of polymerization between crosslink points and $B$ is a constant which depends on the polymer/solvent system. From Eqs. (28.26) and (28.28) it follows that

$$G=B\varphi_e^n, \quad (28.29)$$

where $n=3\nu/(3\nu-1)$. Eq. (28.29) predicts that the concentration dependence of the elastic moduli of gel homologs (chemically similar gels having different crosslinking densities) follows a simple power law behavior. The value of $n$ depends on the thermodynamic quality of the solvent: in good solvent condition $n\simeq 2.31$, in theta condition $n=3$.

Here we note that in the simple scaling theory used above, the polymer is considered as an infinitely thin chain possessing length but not volume. At higher polymer concentration, however, the finite volume of the structural elements may no longer be neglected. More recent scaling theories [87,88] using the Flory–Huggins lattice model as a starting point are able to incorporate the polymer volume into their formalism.

***Swelling of Polymer Networks—The Frenkel–Flory–Rehner Hypothesis***

A crosslinked polymer exposed to a thermodynamically compatible diluent absorbs solvent molecules. The driving force of the mixing process is mainly entropic. As the volume increases, the network chains are deformed and an elastic retractive force develops. The chain deformation causes a decrease in the entropy, because the extended configuration of the chains is less probable. Equilibrium is achieved when these opposing forces are balanced.

The basic assumption in the Frenkel–Flory–Rehner theory describing the swelling of a crosslinked polymer is that the elastic ($\Delta F_{el}$) and mixing ($\Delta F_{mix}$) contributions in the free energy that accompany the swelling of the dry network are separable and additive [2,4,5]

$$\Delta F=\Delta F_{el}+\Delta F_{mix}, \quad (28.30)$$

where $\Delta F$ is the total free energy of the polymer-solvent system. At equilibrium with the pure solvent (at constant temperature and pressure) the free energy is at minimum with respect to any changes in composition, i.e.,

$$(\partial\Delta F/\partial n_1)=\mu_1-\mu_1{}^0=0=(\mu_1-\mu_1{}^0)_{mix}+(\mu_1-\mu_1{}^0)_{el}, \quad (28.31)$$

where $n_1$ is the number of moles of solvent, $\mu_1$ is the chemical potential of solvent in the gel and $\mu_1{}^0$ is the chemical potential of the pure solvent. The subscripts $_{mix}$ and $_{el}$ refer to the mixing and elastic contributions to the chemical potential respectively. How the Frenkel–Flory–Rehner model can be used to relate macroscopic swelling

observations to the molecular structure of the network is developed subsequently.

### *Experimental Characterization of Swollen Polymer Networks*

Molecular theories of rubber elasticity (see section on network models) allow the interpretation of the experimental data obtained for elastomeric materials in terms of structural characteristics of the network. The most frequently used experimental techniques are stress-strain measurements and swelling measurements.

#### *Stress-Strain Isotherms*

Uniaxial stress-strain measurements are often used to characterize polymer networks both in the dry state and in equilibrium with a diluent. The analysis of the stress-strain isotherms is usually performed in terms of the reduced force

$$[f^*]=f^*(V_0/V)^{1/3}/(\alpha-\alpha^{-2}), \tag{28.32}$$

where $f^*$ is the force per unit unstrained cross-section of the unswollen network, and $\alpha$ is the deformation ratio relative to the undeformed swollen state of volume $V$. The relationship between $\alpha$ and $\lambda_1$ is given by

$$\lambda_1=\alpha(V/V_0)^{1/3}, \tag{28.33a}$$

and

$$\lambda_2=\lambda_3=\alpha^{-1/2}(V/V_0)^{1/3}. \tag{28.33b}$$

In both the phantom and affine models the reduced force is identified with the elastic modulus. In the affine limit the shear modulus is expressed as

$$G_{\text{aff}}=[f^*]_{\text{aff}}=kT(\nu_{\text{el}}/V_0), \tag{28.34}$$

while in the phantom limit

$$G_{\text{ph}}=[f^*]_{\text{ph}}=kT(\xi/V_0). \tag{28.35}$$

In general, experimental stress-strain isotherms differ from the predictions of the simple statistical theories.

The constrained junction fluctuation theory provides a description of the network behavior which lies between the affine and phantom limits [36,38–40]. According to this theory, the elastic force, $f$, is the sum of two contributions

$$f=f_{\text{ph}}+f_c, \tag{28.36}$$

where $f_{\text{ph}}$ is the phantom network contribution, and $f_c$ arises from the entanglement constraints. The reduced stress $[f^*]$ is given by

$$[f^*]=kT(\xi/V_0)(1+f_c/f_{\text{ph}}). \tag{28.37}$$

The expression for $f_c/f_{\text{ph}}$ in uniaxial deformation is

$$f_c/f_{\text{ph}}=(\mu/\xi)[\lambda K(\lambda_1^2)-\lambda^{-2}K(\lambda_2^2)](\lambda-\lambda^{-2})^{-1}, \tag{28.38}$$

where $\lambda_1=\lambda$ and $\lambda_2=\lambda^{-1/2}$. The function $K$ is defined by

$$K(\lambda_t^2)=B_t[B_t^*(B_t+1)^{-1}+g_t(g_tB_t^*+g_t^*B_t)(g_tB_t+1)^{-1}], \tag{28.39}$$

where $B_t$, $B_t^*$ and $g_t$ are the same as in Eqs. (28.19), (28.21) and (28.22)

The Flory–Erman theory considers topological interactions among junctions and chains only in that they restrict junction fluctuations. Ferry [92], Langley [45], Dossin [46] and Graessley [48] assume that these interactions are also present in the small-strain limit. Dossin and Graessley [46] proposed for the small strain modulus

$$G_0=(\nu_{\text{el}}-h\mu_{\text{el}})kT/V, \tag{28.40}$$

where $h$ is an empirical constant, the value of which is between 0 and 1, depending on the extent to which the junction fluctuations are impeded in the network ($h=0$ in the affine limit, and $h=1$ in the phantom limit).

Gottlieb and Macosko [55] and Gottlieb [49] pointed out that the two parameters $h$ and $\kappa$, both measuring the severity of constraints are related. For the case of a perfect, incompressible, unswollen network the analytical relationship is given by

$$h=1-(1-1/2\zeta)^2\kappa^2(\kappa^2+1)(\kappa+1)^{-4}. \tag{28.40a}$$

At the limit of $\kappa=0$ Eq. (28.40a) yields $h=1$ (phantom network), and at the limit of $\kappa\to\infty$, $h=\zeta(1-\zeta/4)$ and hence for $\zeta=0$ affine network behavior is observed. Affine network behavior is obtained also in the case $\zeta=2$. Intermediate behavior is obtained in ranges of both $0<\kappa<\infty$ and $0<\zeta<2$.

Another approach is to consider that topological interactions raise the free energy of the network, as if there were additional crosslinks [45–48]. The argument is based on the existence of a rubbery plateau modulus, $G_N^0$, which is observed in the viscoelastic properties of high molecular weight linear polymers. The plateau modulus is assumed to be a measure of the entanglement interactions between the chains. In a permanent network the interchain entanglements are fixed due to the presence of the chemical bonds. Langley [45] and Graessley and co-workers [46–48] have suggested that these trapped entanglements can be simply added to the small strain modulus from Eq. (28.40)

$$G=\nu_{\text{el}}kT(1-2h/fT)(V/V_0)^{2/3}/V+T_eG_e^{\max}, \tag{28.41}$$

where $T_e$ is the fraction of the maximum concentration of topological interactions which are permanently trapped by the networks and $G_e^{\max}$ is the maximum possible contribution of entangled chains to the modulus. Thus Eq. (28.41) predicts a small-strain modulus greater than predicted by

the Flory–Erman theory and greater than that of the affine model.

Importantly the Flory–Erman theory has been developed for finite (large) deformations, which is not true of the entanglement model, which resultingly limits the latter's usefulness in terms of making quantitative estimates of experimental results, particularly in large deformation experiments, including swelling.

### *Swelling Measurements*

In addition to mechanical measurements, swelling measurements are frequently used to characterize rubber networks. Of particular interest is the relationship between the molecular weight between crosslinks and the degree of swelling. Unfortunately, the numerical values of the molecular parameters obtained by elastic and swelling measurements strongly depend upon the particular theoretical model used to evaluate the experiments. The model behaviors are described in the following paragraphs.

The swelling equation for a phantom network is given as [44,93]:

$$\ln(1-\varphi_e)+\varphi_e+\chi\varphi_e^2=-(\xi/N_AV_0)V_1\varphi_e^{1/3}, \tag{28.42}$$

while for an affine network [44]

$$\ln(1-\varphi_e)+\varphi_e+\chi\varphi_e^2=-(\xi/N_AV_0)V_1\varphi_e^{1/3}[1+(\mu_{el}/\xi)\times(1-\varphi_e^{2/3})], \tag{28.43}$$

where $N_A$ is Avogadro's number and the extra complexity in Eq. (28.43) arises due to the logarithmic contribution to the free energy in the affine network model [see Eqs. (28.1) and (28.15)].

The corresponding equation according to the Flory–Erman constrained junction fluctuation model is

$$\ln(1-\varphi_e)+\varphi_e+\chi\varphi_e^2=-(\xi/N_AV_0)V_1\varphi_e^{1/3}[1+K(\lambda^2)], \tag{28.44}$$

where $K(\lambda^2)$ has been defined earlier [see Eq. (28.39)].

Queslel *et al.* [93] made a comparison between the values of the molecular network parameters calculated through Eqs. (28.42)–(28.44). The highest value of $M_c$ (chain molecular weight) is obtained by the affine model. The phantom model yields lower $M_c$ than the affine model, because junction fluctuations decrease the impact of the changes in chain entropy in the phantom model. Using Eq. (28.43) the same elastic contribution as that of an affine network is thus achieved if $\xi$ is higher (or correspondingly $M_c$ is smaller). The value of $M_c$ determined from the Flory–Erman model lies between these limiting values. It is important to remark that Eqs. (28.42) and (28.43) enable one to estimate a range for $M_c$ without any prior knowledge of the network structure.

Both the affine and the phantom network models predict that the reduced stress, $[f^*]$, measured in uniaxial deformation is independent of the deformation ratio. However, it became clear from early studies of rubber elasticity that real networks, in general, exhibit significant departures from this prediction: the reduced stress decreases with elongation and also with increasing swelling. It was recognized that the limiting value of the reduced stress at high elongation or swelling ratio is a characteristic quantity of the network.

The detailed calculations according to the constrained junction fluctuation model can only be performed with a computer. The fitting of the stress-strain (or swelling) data to the model, in principle, requires three parameters: $[f^*]_{ph}$, $\kappa$ and $\zeta$. Here we briefly outline the steps of the fitting procedure [94,95]:

1. In many cases it is reasonable to take the initial value of $[f^*]_{ph}=2C_1$, where $2C_1$ is the Mooney–Rivlin constant. An alternative possibility is to estimate $[f^*]_{ph}$ from the stoichiometry of the chemical reaction using Eqs. (28.12)–(28.14) and (28.35).
2. The initial value of $\kappa$ can be obtained from the Flory–Erman theory on the basis of the following argument [94]. Since $\kappa$ is assumed to be proportional to the number of chains sharing the volume occupied by one chain, it is the measure of the degree of interpenetration of the network chains, i.e.,
$$\kappa=I\langle r^2\rangle_0^{3/2}(\nu_{el}/V_0), \tag{28.45}$$
where $\langle r^2\rangle_0$ is the unperturbed dimension of a chain and $I$ is a proportionality constant. Expressing Eq. (28.45) in terms of measurable quantities one gets [94]
$$\kappa=A(2C_1)^{-1/2}\varphi_c^{(4/3)+m}, \tag{28.46}$$
where $\varphi_c$ is the volume fraction of the polymer at crosslinking and $A=I(\langle r^2\rangle_0/M_c)^{3/2}(1-2/f)^{1/2}N_A^{3/2}\varrho^{3/2}(kT)^{1/2}$, where $N_A$ is Avogadro's number, $\rho$ is the density of the polymer, and $f$ is the crosslink functionality. The experimental value of $A$ is the order of unity (for PDMS networks Erman and Mark [95] reported $A=1.29$ and $m=0.385$).
3. In a first approximation the parameter $\zeta$ can be assumed to be zero.
4. Using these initial values the differences between theory and experiment should be minimized. In order to achieve this, the value of $\kappa$ obtained in step (2) is used to calculate $[f^*]_{ph}$ from Eqs. (28.37)–(28.38). Then $2C_1$ in Eq. (28.46) is replaced by $[f^*]_{ph}$ to obtain a new value of $\kappa$. These steps are iterated until $\kappa$ converges. Using the new values of $[f^*]_{ph}$ and $\kappa$ the function $[f^*]$ vs $\alpha^{-1}$ is calculated from Eq. (28.37).
5. The procedure described in 4 is repeated for a new value of $m$ (and $A$), and the values of $[f^*]_{ph}$ and $\kappa$ are recalculated. The calculation is continued until the error between the experimental and the calculated data reaches a minimum.
6. If the agreement between calculated data and experiment is still not perfect, the value of $\zeta$ can be varied to

fit experimental data. The values of $\zeta$ giving the best agreement with experiments are usually close to zero.

## 28.3 ANALYSIS OF EXPERIMENTAL RESULTS

### 28.3.1 General Comments

The primary goal of the molecular theories is to derive the structure-property relationships for polymeric networks. A quantitative understanding of the dependence of the physical properties upon the network structure is essential to deduce molecular parameters (e.g., molecular weight between crosslinks) from measurements. This is also required to synthesize new polymer networks having desired physical properties.

To test the validity of different network theories is particularly difficult because the structure of the network is unknown at the molecular level. Usually crosslinks are introduced in a less perfectly controlled manner than desired. The extent of imperfections depends on the mechanism of the crosslinking process, e.g., clustering of chains or junctions may lead to deviations from the complete randomness assumed in the theories. In most cases, the distribution of the network chains and junctions is not uniform throughout the sample.

Analysis of the experimental data obtained for model networks having known structure provides a straightforward way of understanding the structure-property relationships. Such model networks can be synthesized by specific chemical reactions, e.g., by end-linking of well characterized polymer chains through a controlled chemical reaction. The characteristics of the chains, prior to crosslinking, can be determined using the usual solution characterization techniques (gel chromatography, viscometry, etc.). In this way the average molecular weight between crosslinks ($M_c$) and the distribution of $M_c$ can be varied in a controlled manner. The crosslink functionality ($f$) is known from the chemistry of the crosslinking reaction. Since $\nu_{el}$ and $f$ are known $\xi=\nu_{el}-\mu_{el}+1$ is also known. Assuming that the chemical reaction between the end-groups of the chains and the crosslinking agent is stoichiometric, and that the effects of entanglements and network imperfections (cycles, pendent chains) are negligible, the elastic properties of the gel can be predicted. Equations (28.34) and (28.35) allow the elastic modulus both in the phantom and the affine limits to be calculated. The decrease of the modulus with $\lambda$ depends on the values of $\kappa$ and $\zeta$ in the Flory–Erman theory. Unfortunately, this theory does not make an a priori prediction for these parameters. Since no independent information is available about the actual size of the junction fluctuation domains and about the anisotropy of these domains, the values of $\kappa$ and $\zeta$ can only be determined empirically using a fitting procedure such as that described in the section on swelling measurements.

The testing of the network models with regard to the prediction of the equilibrium swelling degree of the crosslinked polymer as a function of the thermodynamic activity of the diluent requires further assumptions concerning the mixing free energy contribution. This term is supposed, firstly, to be separable from the total change in the free energy [see Eq. (28.30)] and, secondly, to be identical for the gel and for the solution of the uncrosslinked polymer of infinite molecular weight. The latter assumption presumes that the polymer-solvent interaction parameter is unaffected by the presence of crosslinks. Thus, the only difference between the swollen network and the polymer solution is the existence of a permanent elastic modulus and the theoretical dependence of the equilibrium volume fraction upon the molecular parameters is predicted by Eqs. (28.42)–(28.44).

The structure of any real network exhibits departures from that of the ideal (model) network. A comparison between the experimental and theoretical values of the network parameters provides quantitative information on the deviation from the behavior of the hypothetical model system, and allows one to treat real networks by reference to the structural parameters of a perfect network. In the following sections, typical experimental results obtained for different network systems and analyzed using different theoretical approaches are briefly reviewed.

### 28.3.2 Determination of the Model Parameters from Stress-Strain Measurements

A large amount of experimental work has been reported on the stress-strain behavior of swollen polymeric networks. Fitting of stress-strain data measured at different degrees of dilution to Eqs. (28.37)–(28.39) enables one to determine $\xi$, $\kappa$ and $\zeta$.

Erman and Flory [39] reanalyzed the data of Allen *et al.* [96] on swollen natural rubber samples crosslinked with dicumyl peroxide. It was found that the shape of the $[f^*]$ vs. $\alpha^{-1}$ curves in a wide range of dilution in $n$-decane ($0.24<\varphi<1$) can be well reproduced using a single set of parameters $[f^*]_{ph}=0.166$ MPa, $\kappa=8$ and $\zeta=0.12$. Similar analysis of the data of Flory and Tatara [33] for radiation crosslinked PDMS samples swollen in benzene yields the values $[f^*]_{ph}=0.136$ MPa, $\kappa=6$ and $\zeta=0.12$. For poly(ethyl acrylate) networks [37] having different crosslink densities swollen in bis(2-ethoxyethyl)ether $\kappa$ varied in the range 1.8–16.0, and $\zeta$ varied between 0.0 and 0.1. It was also found that the stress-strain isotherms for the same networks in the unswollen state and in swelling equilibrium with a diluent are consistently described by the same set of parameters, $\kappa$ and $\zeta$. Typical $[f^*]$ vs $\alpha^{-1}$ data along with the fit of the Flory–Erman theory are shown in Fig. 28.5.

Swelling equilibrium measurements provide an independent route to determine $[f^*]_{ph}$. At swelling equilibrium the sum of the contributions to the chemical potential from mixing and from the elastic deformation of the network should be zero [see Eq. (28.31)]. Thus

$$0=\ln(1-\varphi)+\varphi+\chi\varphi^2+(V_1\xi/N_AV_0)\lambda^{-1}[1+K(\lambda^2)], \tag{28.47}$$

where $N_A$ is the Avogadro number. Substitution for $\xi/V_0$ according to Eq. 28.35 yields

$$[f^*]_{ph}=-(RT/V_1)[\ln(1-\varphi)+\varphi+\chi\varphi^2]\lambda/[1+K(\lambda^2)], \tag{28.48}$$

where $K(\lambda^2)$ is defined by Eq. (28.39).

Using Eq. (28.48) Erman and Flory [39] analyzed the results of Mark and Sullivan [97] on end-linked PDMS networks swollen in benzene as well as the data from Erman, Wagner and Flory [37] on poly(ethyl acrylate). They compared the values of $[f^*]_{ph}$ obtained from stress-strain isotherms and swelling measurements with data calculated from the chemistry of cross-linking. The $[f^*]_{ph}$ values derived from elasticity measurements were slightly higher than those calculated from the known molecular weights of the primary chains on the basis of stoichiometry. The deviation was attributed to possible departures from equilibrium in the force measurements. The most pronounced departure was observed for networks of low degrees of crosslinking in which the approach to equilibrium is protracted. No such deviation was detected for $[f^*]_{ph}$ obtained from swelling measurements. The satisfactory agreement between the experimental and the calculated values of $[f^*]_{ph}$ led the authors to the conclusion that trapped entanglements do not have a significant contribution to the elastic response of the network. If the effective degree of interlinking is enhanced by discrete entanglements, the values of $[f^*]_{ph}$ deduced from elastic or swelling measurements should exceed the chemical values of $kT\xi/V_0$ calculated from the chemistry of crosslinking.

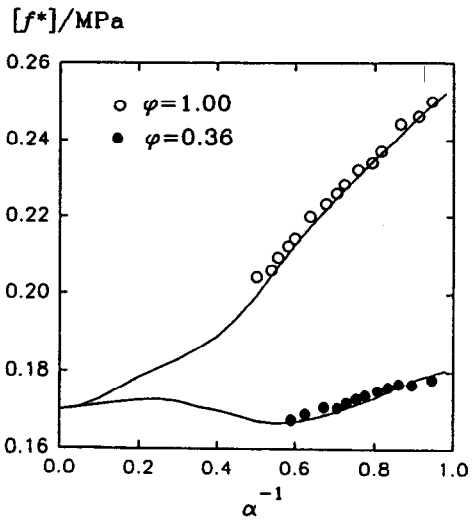


**FIGURE 28.5.** "Mooney–Rivlin" reduced stress plot showing comparison of experimental data with modified constrained chain model (MCC) predictions for dry (○) and swollen (●) natural rubber networks [96,102]. Swelling agent: *n*-Decane. Continuous lines are theoretical curves calculated with parameters $\xi kT/V_0=0.17$ MPa and $\kappa_G=2.0$.

Gottlieb *et al.* [54] reached a conclusion opposite that drawn by Erman and Flory by the analysis of data on PDMS from different sources, including the same data set of Mark and Sullivan [97]. They argued that trapped entanglements contribute substantially to the stress. Erman and Flory [39] criticized this interpretation on several grounds. Their main criticism was that Gottlieb *et al.* [54] confined attention to stresses at small strains and did not deduct the contribution to the reduced stress from restraints on junction fluctuations. In the analysis of Gottlieb *et al.*, such fluctuations are assumed to be totally suppressed at small strains, as if $\kappa=\infty$ for all networks, and the contribution arising from the constraints is treated as a constant fraction of the reduced stress. This procedure may enhance the reduced forces by factors that increase with decreasing crosslink density, and lead to a finite value of $[f^*]_{ph}$ at $\xi=0$. According to Flory and Erman [39] the large entanglement contribution in the analysis conducted by Gottlieb *et al.* [54] is largely a fiction of their data treatment.

A comprehensive analysis of previously reported stress-strain data for five different elastomers both in the swollen and unswollen states was performed on the basis of the Flory–Erman theory by Brotzman and Mark [98] (Table 28.1). They found that in most cases, as the polymer volume fraction decreases, the value of $\kappa$ required to describe the experimental data also decreases. The analysis also revealed that when $\zeta$ is set to zero, the high-extension intercept of the $[f^*]_{ph}$ vs $\alpha^{-1}$ curves is practically independent of the degree of swelling. In Table 28.2, the values of $2C_1$ and $2C_1+2C_2$ obtained for the same networks by using the linear Mooney–Rivlin equation of the reduced force, $[f^*]=2C_1+2C_2\alpha^{-1}$, are listed. The $2C_1$ values are in reasonable agreement with the $[f^*]_{ph}$ data given in Table 28.1, indicating that the Mooney–Rivlin treatment can yield similar estimates of the cycle rank of the network as does the more detailed theoretical approach.

Poorer agreement was found between $[f^*]_{ph}$ and $2C_1$ by Sharaf and Mark [99]. These authors re-examined the small-strain modulus data reported for unswollen PDMS model networks (Table 28.3). The values $[f^*]_{ph}$ were found two- or threefold lower than the corresponding values of $2C_1$. For comparison in Table 28.4, the characteristic quantities of the same PDMS model networks are given in terms of the entanglement model [see Eqs. (28.40) and (28.41)].

The constrained junction fluctuation theory of amorphous polymer networks was modified by Erman and Monnerie [100]. The fundamental difference between the modified and the original models is the adoption of the assumption that constraints affect the whole chain rather than the junction points only. They considered two different cases: (1) the fluctuations of all points along the chains in the phantom network are independent of macroscopic strain (constrained chain scheme, CC); and (2) the fluctuations of the points in the phantom network are dependent on the macroscopic

**TABLE 28.1.** *Parameters of the stress-strain isotherms calculated from the fit of the Flory–Erman model for different networks systems [98].*

| Polymer[a] | Diluent | $f$ | Cross-linker | T/°C | $\varphi$ | $[f^*]_{ph}$/MPa | $\kappa$ | $\zeta$ |
|---|---|---|---|---|---|---|---|---|
| PDMS [111] | lin. PDMS | 4 | $\gamma$-irradiation | 30 | 1.00 | 0.0325 | 7.66 | 0.00 |
| | | | | | 0.80 | 0.0317 | 4.79 | 0.00 |
| | | | | | 0.60 | 0.0317 | 4.10 | 0.00 |
| | | | | | 0.40 | 0.0318 | 3.96 | 0.00 |
| | | | | | 1.00 | 0.0355 | 6.75 | 0.05 |
| | | | | | 0.80 | 0.334 | 4.91 | 0.05 |
| | | | | | 0.60 | 0.0330 | 5.02 | 0.05 |
| | | | | | 0.40 | 0.0333 | 4.69 | 0.05 |
| | | | | | 1.00 | 0.0366 | 6.94 | 0.10 |
| | | | | | 0.80 | 0.0341 | 6.09 | 0.10 |
| | | | | | 0.40 | 0.0343 | 9.96 | 0.10 |
| PDMS [111] | lin. PDMS | 4 | $\gamma$-irradiation | 30 | 1.00 | 0.0245 | 14.3 | 0.00 |
| | | | | | 0.80 | 0.0238 | 4.74 | 0.00 |
| | | | | | 0.60 | 0.0232 | 4.63 | 0.00 |
| | | | | | 0.40 | 0.0221 | 4.35 | 0.00 |
| PDMS [111] | lin. PDMS | 4 | $\gamma$-irradiation | 30 | 1.00 | 0.0146 | 15.3 | 0.00 |
| | | | | | 0.80 | 0.0139 | 8.23 | 0.00 |
| | | | | | 0.60 | 0.0129 | 10.8 | 0.00 |
| | | | | | 0.40 | 0.0130 | 4.77 | 0.00 |
| PBD-S [112] | 1,2,4-tri-chloro-benzene | 4 | 1% sulfur | 25 | 1.00 | 0.222 | 7.93 | 0.00 |
| | | | | | 0.80 | 0.213 | 6.43 | 0.00 |
| | | | | | 0.60 | 0.204 | 6.74 | 0.00 |
| | | | | | 0.40 | 0.192 | 8.07 | 0.00 |
| | | | | | 0.20 | 0.212 | 5.21 | 0.00 |
| | | | | | 1.00 | 0.245 | 6.83 | 0.05 |
| | | | | | 0.80 | 0.232 | 6.04 | 0.05 |
| | | | | | 0.60 | 0.227 | 5.47 | 0.05 |
| | | | | | 0.40 | 0.219 | 7.68 | 0.05 |
| | | | | | 0.20 | 0.231 | 12.0 | 0.05 |
| | | | | | 1.00 | 0.250 | 10.3 | 0.10 |
| | | | | | 0.80 | 0.237 | 7.77 | 0.10 |
| | | | | | 0.60 | 0.232 | 8.12 | 0.10 |
| | | | | | 0.40 | 0.229 | 25.0 | 0.10 |
| | | | | | 0.20 | 0.240 | 4.81 | 0.10 |
| PBD-G [112] | 1,2,4-tri-chloro-benzene | 4 | $\gamma$-irradiation | 10 | 1.00 | 0.107 | 20.2 | 0.00 |
| | | | | | 0.80 | 0.097 | 16.4 | 0.00 |
| | | | | | 0.60 | 0.98 | 9.77 | 0.00 |
| | | | | | 0.40 | 0.93 | 8.11 | 0.00 |
| | | | | | 0.20 | 0.93 | 6.78 | 0.00 |
| | | 24 | | 10 | 1.00 | 0.162 | 24 | 0.00 |
| | | | | | 0.80 | 0.135 | 20 | 0.00 |
| | | | | | 0.60 | 0.127 | 22.8 | 0.00 |
| | | | | | 0.40 | 0.111 | 27.2 | 0.00 |
| | | | | | 0.20 | 0.101 | 29.7 | 0.00 |
| PBDP-P [112] | 1,2,4-tri-chloro-benzene | 4 | 1% benzoyl peroxide | 10 | 1.00 | 0.147 | 2.96 | 0.00 |
| | | | | | 0.80 | 0.143 | 2.16 | 0.00 |
| | | | | | 0.60 | 0.142 | 1.42 | 0.00 |
| | | | | | 0.40 | 0.142 | 0.84 | 0.00 |
| | | | | | 0.20 | 0.140 | 1.07 | 0.00 |
| | | 24 | | 10 | 1.00 | 0.164 | 18.2 | 0.00 |
| | | | | | 0.80 | 0.153 | 16.1 | 0.00 |
| | | | | | 0.60 | 0.143 | 17.7 | 0.00 |
| | | | | | 0.40 | 0.138 | 25.4 | 0.00 |
| | | | | | 0.20 | 0.136 | 23.0 | 0.00 |
| PIB [113] | 1,2,4-tri-chloro-benzene | 4 | disulfide | 30 | 1.00 | 0.082 | 10.0 | 0.00 |
| | | | | | 0.80 | 0.083 | 2.44 | 0.00 |

**TABLE 28.1.** *Continued.*

| Polymer | Diluent | $f$ | Cross-linker | T/°C | $\varphi$ | $[f^*]_{ph}$/MPa | $\kappa$ | $\zeta$ |
|---|---|---|---|---|---|---|---|---|
| | | | | | 0.60 | 0.073 | 3.98 | 0.00 |
| | | | | | 0.40 | 0.070 | 2.65 | 0.00 |
| | | | | 20 | 1.00 | 0.166 | 3.22 | 0.00 |
| | | | | | 0.80 | 0.104 | 3.74 | 0.00 |
| | | | | | 0.60 | 0.104 | 2.75 | 0.00 |
| | | | | | 0.40 | 0.095 | 3.14 | 0.00 |
| | | | | 15 | 1.00 | 0.131 | 3.95 | 0.00 |
| | | | | | 0.80 | 0.123 | 4.11 | 0.00 |
| | | | | | 0.60 | 0.119 | 2.16 | 0.00 |
| | | | | | 0.40 | 0.107 | 1.21 | 0.00 |
| POE [114] | phenyl-acetate | 3 | triisocyanate | 25 | 1.00 | 0.721 | 1.14 | 0.00 |
| | | | | | 0.597 | 0.637 | 1.58 | 0.00 |
| | | | | | 0.565 | 0.549 | 2.26 | 0.00 |
| | | | | | 0.488 | 0.337 | 14.8 | 0.00 |
| | | | | | 0.390 | 0.608 | 1.58 | 0.00 |
| POE [114] | phenyl-acetate | 3 | triisocyanate | 25 | 0.429 | 0.608 | 1.56 | 0.00 |
| | | | | | 0.325 | 0.240 | 2.52 | 0.00 |
| | | | | | 0.220 | 0.259 | 0.960 | 0.00 |
| POE [114] | phenyl-acetate | 3 | triisocyanate | 25 | 0.457 | 0.314 | 1.29 | 0.00 |
| | | | | | 0.341 | 0.345 | 1.19 | 0.00 |
| | | | | | 0.291 | 0.314 | 1.29 | 0.00 |
| | | | | | 0.488 | 0.337 | 14.8 | 0.00 |
| | | | | | 0.390 | 0.608 | 1.58 | 0.00 |
| POP [115] | benzene | | tris(p-phenyl-misocyanate) thiophosphate | 60 | 0.216 | 0.285 | 2.0 | 0.00 |
| | | | | | 0.216 | 0.315 | 2.2 | 0.00 |
| | | | $M_c$=3000 | | 0.286 | 0.400 | 1.5 | 0.00 |
| | | | $M_c$=2000 | | 0.286 | 0.417 | 1.7 | 0.00 |
| | | | | | 0.273 | 0.376 | 1.7 | 0.00 |
| | | | $M_c$=1025 | | 0.406 | 0.805 | 0.5 | 0.00 |
| | | | | | 0.421 | 0.773 | 0.5 | 0.00 |
| | | | $M_c$=725 | | 0.464 | 0.750 | 0.5 | 0.00 |
| | | | | | 0.456 | 0.769 | 0.5 | 0.00 |
| | | | $M_c$=730 | | 0.473 | 0.725 | 0.4 | 0.00 |
| | | | | | 0.477 | 0.758 | 0.4 | 0.00 |
| | | | | | 0.440 | 0.755 | 0.4 | 0.00 |
| | | | $M_c$=740 | | 0.522 | 0.695 | 0.5 | 0.00 |
| | | | | | 0.519 | 0.645 | 0.4 | 0.00 |
| | | | $M_c$=725 | | 0.480 | 0.850 | 0.5 | 0.00 |
| | | | | | 0.510 | 0.829 | 0.4 | 0.00 |

[a]PDMS: poly(dimethyl siloxane); PDB: cis-1,4-polybutadiene; PIB: polyisobutylene; POE: poly(oxyethylene); POP: poly(oxypropylene).

strain, only the junctions are invariant to strain (modified constrained chain scheme, MCC). The important consequence is that $\kappa$ of the constrained junction fluctuation theory has been replaced by the function [100]

$$h(\lambda_1)=\kappa_G[1+(\lambda_1^2-1)\Phi]^{-1}, \qquad (28.49)$$

where $\kappa_G$ is a parameter corresponding to $\kappa$, and

$$\Phi=(1-2/f)^2/3 \quad \text{(CC model)}, \qquad (28.50a)$$

$$\Phi=(1-2/f)^2 \quad \text{(MCC model)}. \qquad (28.50b)$$

Both constrained chain models predict that the elastic modulus may exceed the value obtained from the affine model, and according to the MCC scheme it exhibits a more sensitive dependence upon elongation or swelling than given by the original Flory–Erman theory. The effect of constraints is represented by a single parameter $\kappa_G$ instead of the two parameters $\kappa$ and $\zeta$ in the previous model, which makes the new theory more straightforward for the interpretation of the experimental stress-strain-swelling data.

Fontaine *et al.* [101,102] compared the prediction of the constrained chain models with the results of elongation measurements performed on dry and swollen natural rubber, poly(ethylene oxide), polybutadiene, poly(dimethylsiloxane) and cis-1,4-polyisoprene networks. In Table 28.5 the parameters obtained by analysis of the same network systems using both the CC and the MCC models are listed. It was found that the strong dependence of the reduced

**TABLE 28.2.** *Mooney-Rivlin parameters of the stress-strain isotherms for different networks systems [98].*

| Polymer | Diluent | $f$ | Cross-linker | $T$/°C | $\varphi$ | $2C_1$/MPa | $(2C_1+2C_2)$/MPa |
|---|---|---|---|---|---|---|---|
| PDMS [111] | lin. PDMS | 4 | $\gamma$-irradiation | 30 | 1.00 | 0.0304 | 0.0571 |
| | | | | | 0.80 | 0.0298 | 0.0476 |
| | | | | | 0.60 | 0.0299 | 0.0433 |
| | | | | | 0.40 | 0.0305 | 0.0398 |
| PDMS [111] | lin. PDMS | 4 | $\gamma$-irradiation | 30 | 1.00 | 0.0218 | 0.0533 |
| | | | | | 0.80 | 0.0220 | 0.0365 |
| | | | | | 0.60 | 0.0218 | 0.0324 |
| | | | | | 0.40 | 0.0208 | 0.0290 |
| PDMS [111] | lin. PDMS | 4 | $\gamma$-irradiation | 30 | 1.00 | 0.0118 | 0.0364 |
| | | | | | 0.80 | 0.0121 | 0.0255 |
| | | | | | 0.60 | 0.0117 | 0.0230 |
| | | | | | 0.40 | 0.0126 | 0.0168 |
| PBD-S [112] | 1,2,4,-tri-chloro-benzene | 4 | 1% sulfur | 25 | 1.00 | 0.203 | 0.406 |
| | | | | | 0.80 | 0.202 | 0.343 |
| | | | | | 0.60 | 0.202 | 0.302 |
| | | | | | 0.40 | 0.196 | 0.272 |
| | | | | | 0.20 | 0.204 | 0.254 |
| PBD-G [112] | 1,2,4-tri-chloro-benzene | 4 | $\gamma$-irradiation | 10 | 1.00 | 0.0904 | 0.280 |
| | | | | | 0.80 | 0.0864 | 0.210 |
| | | | | | 0.60 | 0.0915 | 0.167 |
| | | | | | 0.40 | 0.0933 | 0.135 |
| | | | | | 0.20 | 0.0878 | 0.117 |
| | | 24 | | 10 | 1.00 | 0.0904 | 0.28 |
| | | | | | 0.80 | 0.0868 | 0.210 |
| | | | | | 0.60 | 0.0915 | 0.167 |
| | | | | | 0.40 | 0.0933 | 0.135 |
| | | | | | 0.20 | 0.0878 | 0.117 |
| PBD-P [112] | 1,2,4-tri-chloro-benzene | 4 | 1% benzoyl peroxide | 10 | 1.00 | 0.142 | 0.228 |
| | | | | | 0.80 | 0.140 | 0.178 |
| | | | | | 0.60 | 0.138 | 0.160 |
| | | | | | 0.40 | 0.138 | 0.150 |
| | | | | | 0.20 | 0.142 | 0.144 |
| | | 24 | | 10 | 1.00 | 0.164 | 0.168 |
| | | | | | 0.80 | 0.140 | 0.178 |
| | | | | | 0.60 | 0.138 | 0.160 |
| | | | | | 0.40 | 0.138 | 0.150 |
| | | | | | 0.20 | 0.135 | 0.144 |
| PIB [113] | 1,2,4-tri-chloro-benzene | 4 | disulfide | 30 | 1.00 | 0.072 | 0.159 |
| | | | | | 0.80 | 0.083 | 0.103 |
| | | | | | 0.60 | 0.074 | 0.0953 |
| | | | | | 0.40 | 0.073 | 0.0777 |
| | | | | 20 | 1.00 | 0.113 | 0.165 |
| | | | | | 0.80 | 0.0976 | 0.148 |
| | | | | | 0.60 | 0.104 | 0.131 |
| | | | | | 0.40 | 0.0905 | 0.115 |
| | | | | 15 | 1.00 | 0.128 | 0.194 |
| | | | | | 0.80 | 0.123 | 0.170 |
| | | | | | 0.60 | 0.114 | 0.145 |
| | | | | | 0.40 | 0.108 | 0.114 |
| POE [114] | phenyl-acetate | 3 | triisocyanate | 25 | 1.00 | 0.744 | 0.934 |
| | | | | | 0.597 | 0.660 | 0.795 |
| | | | | | 0.565 | 0.613 | 0.722 |
| | | | | | 0.488 | 0.575 | 0.732 |
| | | | | | 0.390 | 0.593 | 0.715 |
| POE [114] | phenyl-acetate | 3 | triisocyanate | 25 | 0.429 | 0.251 | 0.320 |
| | | | | | 0.325 | 0.231 | 0.296 |
| | | | | | 0.220 | 0.263 | 0.266 |

**TABLE 28.2.** *Continued.*

| Polymer | Diluent | $f$ | Cross-linker | $T$/°C | $\varphi$ | $2C_1$/MPa | $(2C_1+2C_2)$/MPa |
|---|---|---|---|---|---|---|---|
| POE [114] | phenyl-acetate | 3 | triisocyanate | 25 | 0.457 | 0.280 | 0.390 |
| | | | | | 0.341 | 0.329 | 0.402 |
| | | | | | 0.291 | 0.310 | 0.348 |
| POP [115] | benzene | | tris(*p*-phenyl-isocyanate) thiophosphate | 60 | 0.216 | 0.322 | 0.423 |
| | | | | | 0.216 | 0.328 | 0.477 |
| | | | $M_c$=3000 | | 0.286 | 0.450 | 0.546 |
| | | | $M_c$=2000 | | 0.286 | 0.448 | 0.594 |
| | | | | | 0.273 | 0.398 | 0.537 |
| | | | $M_c$=1025 | | 0.406 | 0.839 | 0.899 |
| | | | | | 0.421 | 0.839 | 0.859 |
| | | | $M_c$=725 | | 0.464 | 0.810 | 0.835 |
| | | | | | 0.456 | 0.847 | 0.851 |
| | | | $M_c$=730 | | 0.473 | 0.779 | 0.785 |
| | | | | | 0.477 | 0.796 | 0.832 |
| | | | | | 0.440 | 0.814 | 0.817 |
| | | | $M_c$=740 | | 0.522 | 0.723 | 0.776 |
| | | | | | 0.519 | 0.647 | 0.713 |
| | | | $M_c$=725 | | 0.480 | 0.861 | 0.959 |
| | | | | | 0.510 | 0.891 | 0.904 |

force on extension and swelling, observed in all the experiments, can be satisfactorily described by the constrained chain models. The value of the parameter, $\kappa_G$, varies between 0.9 and 6.0 for all five network systems investigated. (The other parameter, $\xi kT/V_0$, required to describe the strain and swelling dependence of the data is obtained

**TABLE 28.3.** *Parameters of the stress-strain isotherms calculated from the Flory–Erman model for unswollen PDMS model networks [99].*

| $M_n$(g mol$^{-1}$) | $f$ | $[f^*]_{ph}$/Mpa | $\kappa$ | $2C_1$/MPa | $2C_2$/MPa |
|---|---|---|---|---|---|
| 32900 | 3 | 0.013 | 19.4 | 0.033 | 0.034 |
| 25600 | 3 | 0.014 | 18.2 | 0.043 | 0.052 |
| 18500 | 3 | 0.021 | 15.0 | 0.066 | 0.061 |
| 9500 | 3 | 0.053 | 9.5 | 0.093 | 0.057 |
| 4700 | 3 | 0.075 | 7.9 | 0.148 | 0.011 |
| 4000 | 3 | 0.101 | 6.8 | 0.192 | 0.015 |
| 45000 | 4 | 0.008 | 22.3 | 0.038 | 0.030 |
| 32900 | 4 | 0.015 | 16.4 | 0.058 | 0.042 |
| 25600 | 4 | 0.028 | 11.9 | 0.084 | 0.055 |
| 18500 | 4 | 0.023 | 13.3 | 0.089 | 0.040 |
| 9500 | 4 | 0.062 | 8.0 | 0.167 | 0.050 |
| 4700 | 4 | 0.119 | 5.8 | 0.353 | 0.031 |
| 4000 | 4 | 0.195 | 4.5 | 0.395 | 0.021 |
| 18500 | 4 | 0.020 | 14.3 | 0.096 | 0.043 |
| 18500 | 4 | 0.020 | 14.3 | 0.089 | 0.043 |
| 18500 | 4 | 0.020 | 14.3 | 0.089 | 0.040 |
| 11300 | 4 | 0.082 | 7.0 | 0.196 | 0.083 |
| 11300 | 4 | 0.079 | 7.1 | 0.169 | 0.115 |
| 11300 | 4 | 0.084 | 6.9 | 0.199 | 0.076 |
| 11300 | 4 | 0.064 | 7.9 | 0.188 | 0.092 |
| 11300 | 4 | 0.060 | 8.2 | 0.178 | 0.098 |
| 11300 | 4 | 0.062 | 8.1 | 0.165 | 0.120 |
| 21500 | 4 | 0.038 | 10.3 | 0.142 | 0.098 |
| 11100 | 4 | 0.086 | 6.8 | 0.207 | 0.087 |
| 8800 | 4 | 0.104 | 6.2 | 0.244 | 0.084 |

**TABLE 28.4.** *Parameters of the stress-strain isotherms for PDMS model networks calculated from the entanglement model $\nu_{el}RT/V$ [54].*

| $M_n$(g mol$^{-1}$) | $f$ | T/K | $10^{-5}$G/Pa | $10^{-5}(\nu RT)$/Pa | $T_e$ |
|---|---|---|---|---|---|
| 32900 | 3 | 298 | 0.699 | 0.286 | 0.467 |
| 25600 | 3 | | 0.947 | 0.377 | 0.474 |
| 18500 | 3 | | 1.27 | 0.508 | 0.467 |
| 9500 | 3 | | 1.50 | 1.41 | 0.641 |
| 4700 | 3 | | 1.59 | 2.00 | 0.467 |
| 4000 | 3 | | 2.07 | 2.66 | 0.536 |
| 45000 | 4 | 298 | 0.68 | 0.185 | 0.278 |
| 32900 | 4 | | 1.00 | 0.335 | 0.38 |
| 25600 | 4 | | 1.40 | 0.618 | 0.571 |
| 18500 | 4 | 298 | 1.29 | 0.517 | 0.324 |
| 9500 | 4 | | 2.17 | 1.38 | 0.466 |
| 4700 | 4 | | 3.84 | 2.63 | 0.439 |
| 4000 | 4 | | 4.16 | 4.185 | 0.625 |
| 18500 | 4 | | 1.35 | 0.45 | 0.278 |
| 11300 | 4 | 298 | 2.79 | 1.72 | 0.744 |
| 11300 | 4 | | 2.84 | 1.68 | 0.723 |
| 11300 | 4 | | 2.75 | 1.77 | 0.769 |
| 11300 | 4 | | 2.75 | 1.50 | 0.804 |
| 11300 | 4 | | 2.76 | 1.41 | 0.752 |
| 11300 | 4 | | 2.85 | 1.44 | 0.771 |
| 21600 | 4 | 298 | 2.40 | 0.871 | 0.774 |
| 11100 | 4 | | 2.94 | 1.87 | 0.866 |
| 8800 | 4 | | 3.28 | 2.28 | 0.783 |

directly from the experimental stress-strain isotherms at $\alpha^{-1}=0$.) In the framework of the Flory–Erman model quantitative agreement between the theory and the data for the polybutadiene and poly(ethylene oxide) networks has been achieved only when both $\kappa$ and the phantom modulus $\xi kT/V_0$ were allowed to be dependent on $\varphi$. The formulation according to the constrained chain models, however, does not require $\varphi$ dependent values of $\xi kT/V_0$ and $\kappa_G$.

### 28.3.3 Determination of the Model Parameters from Swelling Measurements

Swelling of elastomers in a solvent is a relatively simple technique for the characterization of polymer networks. Empirical information, such as the degree of swelling and the elastic modulus, can be obtained by direct measurements. Equilibrium swelling measurements and stress-strain measurements are the most frequently used methods for determining the relative degree of crosslinking. A quantitative analysis of the swelling data, however, requires further considerations.

According to the Frenkel–Flory–Rehner hypothesis, the elastic and mixing contributions to the free energy are additive, and the mixing free energy for the network is the same as that of the corresponding uncrosslinked polymer. It follows from these assumptions that the thermodynamic activity of the solvent in the network contains two separable contributions, $a_{1,c}$ and $a_{1,u}$, representing the diluent activi-

**TABLE 28.5.** *Network parameters calculated by the constrained chain (CC) and modified constrained chain (MCC) models [101,102].*

| System | Cross-linker[a] | $\varphi$ | $(\xi kT/V_0)$/MPa | | $\kappa_G$ | |
|---|---|---|---|---|---|---|
| | | | CC | MCC | CC | MCC |
| *cis* 1,4- | DCP 1.3% | 0.197 | 0.312 | 0.325 | 1.1 | 0.9 |
| polyisoprene/ | DCP 0.75% | 0.165 | 0.215 | 0.220 | 1.6 | 1.6 |
| benzene | DCP 0.30% | 0.133 | 0.115 | 0.125 | 3.0 | 2.5 |
| $T$=25 °C | DCP 0.20% | 0.112 | 0.083 | 0.092 | 3.8 | 3.0 |
| | DCP 0.10% | 0.081 | 0.043 | 0.045 | 5.0 | 6.0 |
| NR/*n*-decane | DCP | 0.24–1.0 | 0.150 | 0.170 | 3.0 | 2.0 |
| PEO/phenylac. | isocyanate | 0.22–1.0 | 0.260 | 0.275 | 1.5 | 1.6 |
| PBD/chl.benz. | sulfur | 0.2–1.0 | 0.235 | 0.235 | 2.0 | 2.6 |
| PDMS/benzene | el.radiation | 0.32–1.0 | 0.125 | 0.135 | 2.5 | 2.0 |

[a]DCP: dicumyl peroxide.

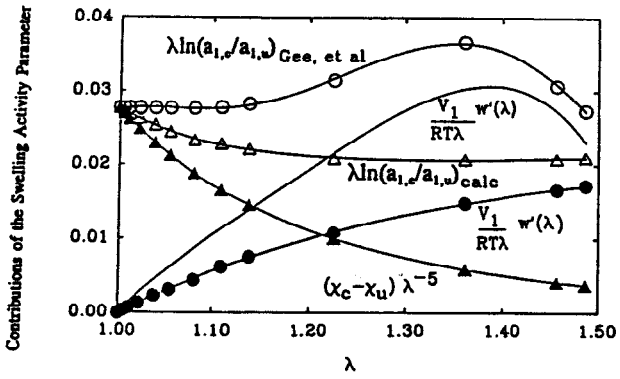


**FIGURE 28.6.** Thermodynamic parameters that contribute to the swelling activity parameter $S$ vs. the swelling deformation $\lambda=\varphi^{-1/3}$. (After Ref. 15. See text for discussion).

ties in the crosslinked and the uncrosslinked polymers, respectively, and the ratio $a_{1,c}/a_{1,u}$ at identical concentrations yields the elastic component of the solvent activity. Experimental tests of this prediction have been performed by differential sorption measurements first conducted by Gee *et al.* [103] In this experiment on a natural rubber/benzene system, the vapor pressure of the solvent and the amount of solvent absorbed by the crosslinked and uncrosslinked rubbers were determined simultaneously by using a sensitive microbalance housed in a vacuum system. Similar experiments were performed by Yen and Eichinger [6], Brotzman and Eichinger [7–9], Neuburger and Eichinger [10], Zhao and Eichinger [11], and McKenna and Crissman [16]. Conventionally the results of these measurements are given in terms of the dimensionless swelling activity parameter [15] (or dilation modulus [6–11])

$$S=\lambda\ \ln(a_{1,c}/a_{1,u}), \tag{28.51}$$

where $\lambda=\varphi^{-1/3}$.

Typical theoretical and experimental $S$ vs. $\varphi^{-1/3}$ curves are shown in Fig. 28.6. The phantom network theory predicts constancy while the affine network model predicts a monotonic increase of $S$ with increasing $\varphi^{-1/3}$. Many of the experimental $S$ vs. $\varphi^{-1/3}$ curves, including that of Gee *et al.* [103] exhibit a maximum. This behavior is consistent with the Flory–Erman theory, although the experimental peak is generally much sharper and significantly greater in magnitude than that predicted by the model. Neuburger and Eichinger [10] determined the swelling activity parameter for poly(dimethylsiloxane) networks in benzene and cyclohexane at 20° and 30 °C. They found that the benzene data at 20 °C can be reasonably well described by the Flory–Erman model with the parameters: $\xi/(N_A V_0)=4.09\times10^{-4}$ mol/cm$^3$, $\kappa=1.0$ and $\zeta=90$ (this value of $\zeta$ is much bigger than that required to fit the stress strain data). The value of the molecular weight between crosslinks, $M_c$, calculated from the equation $\xi/(N_A V_0)=\rho/2M_c$ was $M_c=1190$ g/mol. It is significantly smaller than the actual $M_c=26\,000$ g/mol. Even larger discrepancies were found between the calculated and the actual values of $M_c$ for the PDMS/cyclohexane system. In this case, the best fit was obtained using the phantom network model with $\xi/(N_A V_0)=0.0012$ mol/cm$^3$ corresponding to $M_c=406$ g/mol. The authors concluded that the deviation is the consequence of the breakdown of the Frenkel–Flory–Rehner theory, namely the hypothesis that the elastic and mixing free energies are separable.

McKenna and Crissman [16] performed similar investigations on natural rubber networks swollen in different diluents. They assumed that the elastic free energy contribution is adequately described by the phenomenological Valanis-Landel function [see Eq. (28.1)] and for the measured degree of swelling they calculated it from the values of $w'(\lambda)$ determined in the unswollen state. Comparing these data with the mixing contribution obtained by using Eq. (28.24) they came to the conclusion that the value of the interaction parameter for the crosslinked polymer, $\chi_c$, exceeds that of the solution of the uncrosslinked polymer, $\chi_u$. This conclusion has been supported by lattice model calculations of Freed and Pesci [104], who pointed out that the effective interaction parameter depends on the crosslink density.

McKenna and co-workers [13–16] use the following relation for the swelling activity parameter:

$$S=\lambda\ \ln(a_{1,c}/a_{1,u})=(\chi_c-\chi_u)\lambda^{-5}+V_1 w'(\lambda)/RT\lambda. \tag{28.52}$$

The important point to note from this equation is the assumption that $\chi_c=\chi_u$ often found in the use of the Frenkel–Flory–Rehner hypothesis, has been suppressed. Hence the first term on the right hand side of Eq. (28.52) provides insight into the thermodynamics of swelling and in particular is in accord with the experimental observation that $S\neq0$ as $\lambda\to1$, i.e., no swelling. A typical value for $\chi_c-\chi_u$ of approximately 0.027 can be obtained by examining the curve labeled $\lambda\ln(a_{1,c}/a_{1,u})_{\text{Gee, et al.}}$ of Fig. 28.6 and taking the value at $\lambda=1$.

In Fig. 28.6 we show the thermodynamic parameters from Eq. (28.52) and a comparison with the swelling data of Gee *et al.* [103]. The curve labeled $\lambda\ln(a_{1,c}/a_{1,u})_{\text{Gee, et al.}}$ refers to the data obtained by Gee *et al.* for $S$. The curve labeled $\lambda\ln(a_{1,c}/a_{1,u})_{\text{calc}}$ refers to a calculation of $S$ from Eq. (28.52) using the values of $(\chi_c-\chi_u)\lambda^{-5}$ depicted in the plot on the curve so labeled summed with the values of $V_1 w'(\lambda)/RT\lambda$ determined by measurements on a rubber similar to that used by Gee *et al.* [103] and depicted with solid circles. The solid line without points labeled $V_1 w'(\lambda)/RT\lambda$ represents the value the elastic contribution would have needed to agree with the the Gee *et al.* [103] result. The deviation between the measured and calculated curves is significant, i.e., the crosslink dependence of the interaction parameter does not provide an adequate explanation for the anomalous behavior of the swelling activity

**TABLE 28.6.** *Power law exponents for the concentration dependence of the elastic modulus in swollen network homologs.*

| System[a] | T/°C | $\varphi$ | B/kPa | $n$ | $r^b$ | Refs. |
|---|---|---|---|---|---|---|
| Nr/*n*-decane | 20 | 0.06–0.40 | 4500 | 2.06 | 0.992 | [116,117] |
| PS/benzene | 20 | 0.05–0.20 | 4200 | 2.28 | 0.955 | [105] |
| PS/benzene | 25 | 0.05–0.50 | 4140 | 2.35 | 0.993 | [105] |
| PS/cyclohexane | 37 | 0.12–0.28 | 1750 | 3.14 | 0.980 | [28] |
| PEO/dioxane | 25 | 0.03–0.35 | 8430 | 2.30 | 0.984 | [106] |
| PEO/water | 25 | 0.03–0.30 | 10401 | 2.51 | 0.992 | [106] |
| PHPMA | 25 | 0.08–0.35 | 2590 | 2.59 | 0.995 | [106] |
| PDMS/toluene | 25 | 0.10–0.40 | 2650 | 2.20 | 0.988 | [23] |
| PVAC/toluene | 25 | 0.06–0.30 | 2430 | 2.27 | 0.990 | [22] |
| PVAC/acetone | 25 | 0.05–0.25 | 4420 | 2.25 | 0.992 | [22] |
| PVAC/isopropanol | 70 | 0.10–0.60 | 3388 | 2.31 | 0.977 | [109] |
| PAA/water | 25 | 0.03–0.30 | 4880 | 2.23 | 0.991 | [118] |
| PVA/water | 25 | 0.03–0.30 | 3500 | 2.11 | 0.993 | [116] |

[a]NR: natural rubber; PS: polystyrene; PEO: poly(ethylene oxide); PHPMA: poly(hydroxi-ethyl-methacrylate); PDMS: polydimethylsiloxane; PVAC: poly(vinyl acetate); and PAA: poly(acryamide); PVA: poly(vinyl alcohol).
[b]$r$: Correlation coefficient.

parameter. The reader is referred to McKenna *et al.* [16] for further discussion.

McKenna and Crissman [16] also investigated the effect of temperature on the shape of the $S$ vs. $\varphi^{-1/3}$ curves. In the polyisoprene/benzene system, they did not observe a maximum in $S$ at 30° and 40 °C, rather a rapid decrease occurred which was followed by a plateau region above $\lambda^2=1.2$. At 50 °C, however, a pronounced maximum was found at $\lambda^2=1.13$. Neuburger and Eichinger [10] reported similar changes in the swelling behavior for the PDMS/benzene system in the temperature range between 20° and 30 °C. Similar results were also reported for changing solvent quality by Zhao and Eichinger [11]. Such abrupt changes in behavior imply significant changes in the free energy of the network over a narrow range of temperatures (or solvent qualities). None of the existing network theories predicts such a possibility.

### 28.3.4 Analysis of the Experimental Results on the Basis of the Scaling Theory

The validity of scaling laws has been tested on several swollen network systems (Table 28.6). Munch *et al.* [105] studied the concentration dependence of the shear modulus for polystyrene model networks synthesized by copolymerization of styrene and divinylbenzene and swollen to equilibrium in benzene (good solvent for polystyrene). It was found that the modulus obeys a scaling law with equilibrium concentration, similar to that obtained for semi-dilute polymer solutions. The best fit to the equation $G=B\varphi_e^n$ yields $B=4200$ kPa and $n=2.28$. Hild *et al.* [106] compared the concentration dependence of the shear moduli of poly(ethylene oxide) networks crosslinked by aliphatic pluriisocyanate in two diluents: dioxane and water. The corresponding scaling laws were found: $G=8430\varphi_e^{2.30}$ kPa

**TABLE 28.7.** *Swelling pressure and shear modulus parameters of PVAc networks in toluene and acetone [22].*

| Sample | $\varphi_c$ | A/kPa | $n$ | $p$ | $G_v^e$/kPa | $G_s^e$/kPa |
|---|---|---|---|---|---|---|
| | | | **Toluene 25 °C** | | | |
| 3/50 | 0.089 | 2171 | 2.28 | 0.342 | 8.6 | 8.9 |
| 6/50 | 0.146 | 2613 | 2.29 | 0.331 | 31.6 | 32.4 |
| 6/200 | 0.078 | 2072 | 2.22 | 0.340 | 7.2 | 6.9 |
| 9/50 | 0.208 | 2481 | 2.27 | 0.355 | 70.8 | 70.3 |
| 9/100 | 0.141 | 2350 | 2.25 | 0.336 | 28.6 | 28.3 |
| 9/200 | 0.112 | 2374 | 2.27 | 0.326 | 16.6 | 16.7 |
| 9/400 | 0.074 | 2273 | 2.27 | 0.315 | 6.16 | 6.26 |
| 12/50 | 0.229 | 3100 | 2.35 | 0.383 | 95.7 | 99.8 |
| 12/200 | 0.133 | 2425 | 2.26 | 0.335 | 25.5 | 25.2 |
| | | | **Acetone 25 °C** | | | |
| 9/100 | 0.103 | 4264 | 2.24 | 0.321 | 24.9 | 25.9 |
| 9/200 | 0.078 | 4731 | 2.26 | 0.346 | 14.9 | 14.8 |
| 9/400 | 0.051 | 4262 | 2.24 | 0.369 | 5.44 | 5.24 |

(in 1,4-dioxane) and $G=10400\varphi_e^{2.51}$ kPa (in water). The exponent obtained in 1,4 dioxane is in excellent agreement with the prediction of the scaling theory. However, for the same networks swollen in water, a significantly higher exponent, $n=2.51$, was obtained. They assumed that the deviation from the theoretical exponent is due to the insolubility of the urethane linkages in water, which may induce inhomogeneities in the gels at the molecular level. Hecht and Geissler [107] investigated the elastic properties of polyacryamide gel homologs in a theta solvent (water-methanol mixture, 3:1 by volume). They found that in the concentration range $0.07<\varphi<0.3$ the longitudinal elastic modulus, $E_L$, obtained from light scattering observations, obeys a scaling law $E_L=8090\varphi_e^{3.07}$ kPa in reasonable agreement with the theoretical prediction. Richards and Davidson [108] determined the shear moduli of randomly cross-linked polystyrene networks swollen in cyclohexane at the theta ($\Theta$) temperature (35 °C) and also in toluene (good solvent condition). The power law exponent, $n=3.7$, reported for the theta system exceeds that of the theoretical value. In good solvent conditions (toluene, 20 °C), they found the value $n=2.25$. A comprehensive study of the dependence of the elastic (shear) modulus on the polymer concentration was performed by Zrínyi and Horkay [109] on poly(vinyl acetate) gels swollen to equilibrium in isopropylalcohol. The thermodynamic quality of the solvent was varied by changing the temperature in the range from 30 °C to 70 °C. Isopropylalcohol is a theta solvent for poly(vinyl acetate) at 52 °C and a good solvent at 70 °C. It was found that $G$ vs $\varphi$ exhibits a simple power law behavior at each temperature. The exponent $n$ varies between the values of 2.32 (good solvent condition, 70 °C) and 14.1 (poor solvent condition, 30 °C) [109]. At the theta temperature (52 °C) the best fit to the experimental data yields $n=3.10$.

The osmotic response of swollen polymeric networks was studied on the basis of the scaling theory by Horkay *et al.* [17–19,22,23,110]. They measured both the swelling pressure, $\omega$, and the shear modulus of gels, $G$, at different stages of dilution. The swelling pressure vs polymer volume fraction data were analysed according to the equation [22]

$$\omega=\Pi-G=A\varphi^n-G_v^e(\varphi/\varphi_e)^p, \qquad (28.53)$$

where $\Pi$ is the "osmotic" pressure of the swollen network, $G_v^e$ is the value of the volume elastic modulus at equilibrium with the pure solvent ($\omega=0$) and the constant $A$ depends on the polymer/solvent system. The exponents $n$ and $p$ were iteratively adjusted to minimize the variation of $\omega$ for each set of data points. The resulting values of $A$, $n$, $p$ and $G_v^e$ for poly(vinyl acetate) gels are displayed in Table 28.7. The $n$ values are consistent with the scaling prediction for the mixing term. Also displayed in Table 28.7 are the values of the shear modulus, $G_s^e$, measured at the swelling equilibrium condition. The agreement between the numerical values of the shear and the volume elastic moduli provides experimental evidence that, in highly swollen networks, the separability of the elastic and mixing terms is a reasonable approximation.

## 28.4 SUMMARY

A survey of the thermodynamics and mechanics of crosslinked gels has been presented. Subjects include the phenomenological description of crosslinked networks within the framework of finite elasticity theory and continuum thermodynamics. Particular emphasis is placed on the Valanis–Landel form of the strain energy density function. Several statistical mechanical models of rubber elasticity are also presented. Of particular usefulness are the affine and phantom network models, which are commonly used to derive information about the molecular parameters of the gel from swelling or mechanical measurements. Techniques for using these models and the more modern Flory-Erman constrained junction model and its most recent modifications are described. Experimental data from the literature are presented and used to deduce molecular parameters for the networks using the different models. The application of Scaling Theory to polymer gels is also considered.

Related information can be found in Chapter 23.

## REFERENCES


1. E. Guth and H. Mark, Monatshefte **65**, 93 (1934).
2. P. J. Flory and J. Rehner, J. Chem. Phys. **11**, 521 (1943).
3. H. M. James and E. Guth, J. Chem. Phys. **15**, 651 (1947).
4. P. J. Flory, *Principles of Polymer Chemistry*, (Cornell Univ. Press, Ithaca, NY, 1953).
5. J. Frenkel, Rubber Chem. Technol., **13**, 264 (1940).
6. L. Y. Yen and B. E. Eichinger, J. Polym. Sci. Polym. Phys. Ed. **16**, 121 (1978).
7. R. W. Brotzman and B. E. Eichinger, Macromolecules **14**, 1445 (1981).
8. R. W. Brotzman and B. E. Eichinger, Macromolecules **15**, 531 (1982).
9. R. W. Brotzman and B. E. Eichinger, Macromolecules **16**, 1131 (1983).
10. N. A. Neuburger and B. E. Eichinger, Macromolecules **21**, 3060 (1988).
11. Y. Zhao and B. E. Eichinger, Macromolecules **25**, 6988 (1992).
12. M. Gottlieb and R. J. Gaylord, Macromolecules **17**, 2024 (1984).
13. G. B. McKenna, K. M. Flynn, and Y. Chen, Polym. Commun. **29**, 272 (1988).
14. G. B. McKenna, K. M. Flynn, and Y. Chen, Macromolecules **22**, 4507 (1989).
15. G. B. McKenna, K. M. Flynn, and Y. Chen, Polymer **31**, 1937 (1990).
16. G. B. McKenna and J. M. Crissmann, *Macromolecules 1992*, edited by J. Kahovec, (VSP, Utrecht, The Netherlands 1993) p. 67.
17. F. Horkay and M. Zrinyi, Macromolecules **15**, 1306 (1982).
18. F. Horkay and M. Zrinyi, J. Macromol. Sci. Phys. **B25**, 307 (1986).
19. F. Horkay E. Geissler, A. M. Hecht *et al.*, Macromolecules **21**, 2589 (1988).
20. E. Geissler, F. Horkay, A. M. Hecht *et al.*, J. Chem. Phys. **90**, 1924 (1989).
21. F. Horkay, A. M. Hecht, and E. Geissler, Macromolecules **22**, 2007 (1989).
22. F. Horkay, A. M. Hecht, and E. Geissler, J. Chem. Phys. **91**, 2706 (1989).
23. F. Horkay, M. Zrinyi, E. Geissler *et al.*, Polymer **32**, 835 (1991).
24. F. Horkay, A. M. Hecht, S. Mallam *et al.*, Macromolecules **24**, 2896 (1991).

25. A. M. Hecht, F. Horkay, E. Geissler *et al.*, Macromolecules **24**, 4183 (1991).
26. E. Geissler, F. Horkay, and A. M. Hecht, Macromolecules **24**, 6006 (1991).
27. A. M. Hecht, A. Guillermo, F. Horkay *et al.*, Macromolecules **25**, 3677 (1992).
28. A. M. Hecht, F. Horkay, S. Mallam *et al.*, Macromolecules **25**, 6915 (1992).
29. F. Horkay, W. Burchard, E. Geissler *et al.*, Macromolecules **26**, 1296 (1993).
30. F. Horkay, W. Burchard, A. M. Hecht *et al.*, Macromolecules **26**, 3375 (1993).
31. E. Geissler, F. Horkay, and A. M. Hecht Phys. Rev. Lett. **71**, 645 (1993).
32. J. F. Douglas and G. B. McKenna, Macromolecules **26**, 3282 (1993).
33. P. J. Flory and Y. Tatara, J. Polym. Sci., Polym. Phys. Ed. **13**, 683 (1975).
34. G. Ronca and G. Allegra, J. Chem. Phys. **63**, 4990 (1975).
35. P. J. Flory, Proc. R. Soc. Lond. **A351**, 351 (1976).
36. P. J. Flory, J. Chem. Phys. **66**, 5720 (1977).
37. B. Erman, W. Wagner, and P. J. Flory, Macromolecules **13**, 1554 (1980).
38. P. J. Flory and B. Erman, Macromolecules **15**, 800 (1982).
39. B. Erman and P. J. Flory, Macromolecules **15**, 806 (1982).
40. B. Erman and P. J. Flory, Macromolecules **16**, 1600 (1983).
41. J. E. Mark, Adv. Polym. Sci. **44**, 1 (1982).
42. J. P. Queslel and J. E. Mark, J. Polym. Sci., Polym. Phys. Ed. **22**, 49 (1984).
43. J. P. Queslel and J. E. Mark, Adv. Polym. Sci. **65**, 135 (1984).
44. J. P. Queslel and J. E. Mark, Adv. Polym. Sci. **71**, 229 (1985).
45. N. R. Langley, Macromolecules **1**, 348 (1968).
46. L. M. Dossin and W. W. Graessley, Macromolecules **12**, 123 (1979).
47. D. S. Pearson and W. W. Graessley, Macromolecules **13**, 1001 (1980).
48. W. W. Graessley, Adv. Polym. Sci. **47**, 67 (1982).
49. M. Gottlieb, J. Chem. Phys. **77**, 4783 (1982).
50. G. Marucci, Rheol. Acta **18**, 193 (1979).
51. G. Marucci, Macromolecules **14**, 434 (1981).
52. M. Gottlieb and R. J. Gaylord, Polymer **24**, 1644 (1983).
53. M. Gottlieb, C. W. Macosko, and T. C. Lepsch, J. Polym. Sci., Polym. Phys. Ed. **19**, 1603 (1981).
54. M. Gottlieb, C. W. Macosko, G. S. Benjamin *et al.*, Macromolecules **14**, 1039 (1981).
55. M. Gottlieb and C. W. Macosko, Macromolecules **15**, 535 (1982).
56. D. R. Miller and C. W. Macosko, Macromolecules **9**, 206 (1976).
57. R. J. Gaylord and J. F. Douglas, Polym. Bull. **23**, 529 (1990).
58. R. S. Rivlin, Phil. Trans. R. Soc. **A241**, 379 (1948).
59. L. R. G. Treloar, *The Physics of Rubber Elasticity* (Clarendon, Oxford, 1975).
60. K. C. Valanis and R. F. Landel, J. Appl. Phys. **38**, 2997 (1967).
61. G. B. McKenna and J. A. Hinkley, Polymer **27**, 1368 (1986).
62. E. A. Kearsley and L. Zapas, J. Rheology **24**, 483 (1980).
63. D. F. Jones and L. R. G. Treloar, J. Phys. D. (Appl. Phys.) **8**, 1285 (1975).
64. M. Mooney, J. Appl. Phys. **11**, 582 (1940).
65. W. W. Graessley, Macromolecules **8**, 186 (1975).
66. P. J. Flory, Chem. Rev. **35**, 51 (1944).
67. R. C. Ball, S. F. Edwards, and M. Warner, Polymer **22**, 1010 (1981).
68. R. C. Ball and S. F. Edwards, Macromolecules **13**, 748 (1980).
69. E. A. DiMarzio, J. Chem. Phys. **36**, 1563 (1962).
70. E. A. DiMarzio, Polymer **35**, 1819 (1994).
71. R. T. Deam and S. F. Edwards, Philos. Trans. R. Soc. London A **280**, 378 (1978).
72. S. F. Edwards, Proc. Phys. Soc. **92**, 9 (1967).
73. R. J. Gaylord and J. F. Douglas, Polym. Bull. **18**, 347 (1987).
74. S. F. Edwards and Th. Vilgis, Polymer **27**, 483 (1986).
75. H. G. Kilian, Polymer **22**, 209 (1982).
76. H. F. Enderle and H. G. Kilian, Prog. Coll. Polym. Sci. **75**, 55 (1987).
77. J. Gao and J. H. Weiner, Macromolecules **20**, 2520 (1987).
78. J. Gao and J. H. Weiner, Macromolecules **22**, 979 (1989).
79. B. Deloche and E. T. Samulski, Macromolecules **21**, 3107 (1988).
80. F. T. Wall, J. Chem. Phys. **11**, 527 (1943).
81. P. J. Flory and F. T. Wall, J. Chem. Phys. **19**, 1435 (1951).
82. J. J. Hermans, Trans. Faraday Soc. **43**, 591 (1947).
83. H. M. James and E. Guth, J. Chem. Phys. **15**, 669 (1947).
84. H. M. James and E. Guth, J. Chem. Phys. **21**, 1039 (1953).
85. E. Guth, J. Polym. Sci., Pt. C **12**, 89 (1966).
86. P. J. Flory, British Polym. J. **17**, 96 (1985).
87. M. Muthukumar and S. F. Edwards, J. Chem. Phys. **76**, 2720 (1982).
88. M. Muthukumar, J. Chem. Phys. **85**, 4722 (1986).
89. J. des Cloiseaux, J. Phys. (Les Ulis) **36**, 281 (1973).
90. P. G. de Gennes, *Scaling Concepts in Polymer Physics* (Cornell, Ithaca, NY, 1979).
91. P. J. Flory, Disc. Faraday. Soc. **49**, 7 (1970).
92. J. D. Ferry, Viscoelastic Properties of Polymers (Wiley, New York, 1970).
93. J. P. Queslel, F. Fontaine, and L. Monnerie, Polymer **29**, 1086 (1988).
94. B. Erman and J. E. Mark, Macromolecules **20**, 2892 (1987).
95. B. Erman and J. E. Mark, Macromolecules **25**, 1917 (1992).
96. G. Allen, M. J. Kirkham, J. Padget *et al.*, Trans. Faraday Soc. **67**, 1228 (1971).
97. J. E. Mark and J. L. Sullivan, J. Chem. Phys. **66**, 1006 (1977).
98. R. W. Brotzman and J. E. Mark, Macromolecules **19**, 667 (1986).
99. M. A. Sharaf and J. E. Mark, Polymer **35**, 740 (1994).
100. B. Erman and L. Monnerie, Macromolecules **22**, 3342 (1989).
101. F. Fontaine, C. Morland, C. Noel *et al.*, Macromolecules **22**, 3348 (1989).
102. F. Fontaine, C. Noel, L. Monnerie *et al.*, Macromolecules **22**, 3352 (1989).
103. G. Gee, J. B. M. Herbert, and R. C. Roberts, Polymer **6**, 541 (1965).
104. K. F. Freed and A. I. Pesci, Macromolecules **22**, 4048 (1989).
105. J. P. Munch, S. Candau, J. Herz *et al.*, J. Phys. **38**, 971 (1977).
106. G. Hild, R. Okasha, M. Macret *et al.*, Makromol. Chem. **187**, 2271 (1986).
107. A. M. Hecht and E. Geissler, J. Phys. **39**, 631 (1978).
108. R. W. Richards and N. S. Davidson, Macromolecules **19**, 1381 (1986).
109. M. Zrinyi and F. Horkay, Macromolecules **17**, 2805 (1986).
110. F. Horkay and M. Zrinyi, Macromolecules **21**, 3260 (1988).
111. D. S. Chiu and J. E. Mark, Colloid Polym. Sci. **255**, 644 (1977).
112. D. S. Chiu, T. K. Su, and J. E. Mark, Macromolecules **10**, 1110 (1977).
113. R. R. Rahalkar and J. E. Mark, Polym. J. (Tokyo) **12**, 835 (1980).
114. P. H. Sung and J. E. Mark, J. Polym. Sci. Polym. Phys. Ed. **19**, 507 (1981).
115. A. L. Andrady and M. A. LLorente, J. Polym. Sci. Polym. Phys. Ed. **25**, 195 (1987).
116. F. Horkay and M. Zrinyi, Polym. Bull. **4**, 21, 361 (1981).
117. G. M. Bristow, J. Appl. Polym. Sci. **9**, 1571 (1965).
118. E. Geissler, A. M. Hecht, F. Horkay *et al.*, Macromolecules **21**, 2594 (1988).